From QM to KM

Sergei Viznyuk

Abstract

Understanding of physical reality is rooted in the knowledge obtained from observations. The knowledge is encoded in variety of forms, from sequence of letters in a book, to neural circuits in a brain. At the core, any encoded knowledge is a sample of correlated events (symbols). I show the event samples bear attributes of a physical reality: energy, temperature, momentum, mass. I show that treating measurement as event sampling is consistent with predictions of quantum mechanics (QM). I discuss QM basics: wave function, Born rule, and Schrödinger equation, emphasizing their true meaning, which is rarely, if ever, mentioned in textbooks. I derive similar expressions using event sample as base construct, demonstrating the connection between QM and the presented model. I explain the mechanics of observation, and the role of observer. I show how model extends to include dispersion, decoherence, transition from quantum to classical state. I prove decoherence is a key factor in Fermi's golden rule, in Planck's radiation law, and in emergence of time. The controversial aspects of QM, such as wave function collapse, and measurement problem, do not appear in presented framework, which I call the knowledge mechanics (KM)

As for prophecies, they will pass away; as for tongues, they will cease; as for knowledge, it will pass away.
1 Corinthians 13:8

1. PREAMBLE

Physical properties, such as temperature, energy, entropy, pressure, and phenomena such as Bose-Einstein condensation are exhibited not just by "real" physical systems, but also by virtual entities such as binary or character strings [1, 2, 3], world wide web [4], business and citation networks [5], economy [6, 7]. Quantum mechanical behavior has been observed in objects as different as electrons, electromagnetic waves, nanomechanical oscillators [8]. There must be a mechanism which accounts for the *grand commonality* in observed behavior of vastly different entities. *Scientists have recently discovered that various complex systems have an underlying architecture governed by shared organizing principles* [9]. The *…present-day quantum mechanics is a limiting case of some more unified scheme… Such a theory would have to provide, as an appropriate limit, something equivalent to a unitarily evolving state vector* $|\psi\rangle$ [10].

There are two factors present in all theories. One is the all-pervading *time*, and the other is the observer's *mind*. A successful *grand commonality* model must explain the nature of time, specify mechanism of how the *physical reality* projects onto the mind of observer, and relate time to that projection. Conventional theory routinely manipulates notions, such as energy, distance, electric charge, without providing their definition, treating them as God-given things. A self-contained model must define any notion it operates with. The definition must be confined within the model. A complete theory may not contain underived fundamental physical constants. The conventional QM provides accurate predictions, yet without clear model of the system [11]. This work describes a model wherein state vector formalism for correlated event samples is similar to mathematical apparatus of conventional QM. I expound some notions left obscure by the conventional theory, e.g. the notions of time, of observer, of measurement.

In this preamble I outline the model in defined terms. In Section 2 I develop the concepts of *energy*, of *knowledge*, and of *knowledge confidence*. I calculate energy spectra for some event

samples and show their similarity with known QM constructs: particle in a box, and quantum oscillator. In Section 3, I consider an ensemble of uncorrelated particles. I derive the notion of temperature, and the First Law of Thermodynamics. In Section 4, I discuss conventional QM approach to measurement. I apply state vector formalism to an event sample to obtain Born rule, and Schrödinger equation. I state the equivalence of Born rule and of *coefficient of determination*. I extend formalism to include numeric methods of handling dispersion and decoherence. I show the decoherence is a key factor in Fermi's golden rule, and in Planck's radiation formula. I show how decoherence leads to Second Law of Thermodynamics and to emergence of time.

A description of quantum-level physical reality (*PR*) is attained as a sample $\{n_i\}$ of eigenstates $\{\boldsymbol{i}\} \in \boldsymbol{G}$, where $\boldsymbol{G}$ is a set of eigenstates *PR* can be observed in. In information terms, the eigenstate is an *event*; n_i is the number of occurrences of $\boldsymbol{i}$-th event in the sample. The acquisition of a sample is *measurement*. The sample is encoded in an information-holding construct, which I call the *observer*. The event is *elementary* if it is not a direct product of other events. I call event a *particle*, in some contexts. The particles are said to be *entangled* if they are parts of a non-elementary event.

The event sample describes a quantum object, if events sampled in different observation bases are correlated. An ensemble of uncorrelated particles represents a classical object.

I call a variation of observation basis the *transformation*. A transformation is correlative with a change in macroscopic parameters, notably *time*, *position*, etc. I call a change of eigenstate population numbers $\{n_i\}$, associated with transformation, the *transition*.

The quantitative measure of information (*knowledge*), about object, is obtained from event sample $\{n_i\}$, as a difference between entropy of *equilibrium* (maximum probability state), and entropy of statistical ensemble $\{n_i\}$. The calculation is based on understanding of entropy as a measure of *missing information* (i.e. the amount of *unknown*). The sum of knowledge (i.e. the amount of *known*), and amount of *unknown* equals entropy of equilibrium.

All graphs have been pushed to the end of the paper to make text part more focused. This paper is a substantial re-write of its predecessor [12], most significantly in Section 4.

2. ENERGY

The unconditional probability of an event sample $\{n_i\}$ is given by multinomial probability mass function (*pmf*):

$$P\big((n_i);\ N,(p_i)\big) = N! \prod_{\boldsymbol{i}\in\boldsymbol{G}} \frac{p_i^{n_i}}{n_i!} \tag{1}$$

, where p_i is the probability of sampling eigenstate $\boldsymbol{i}$ from set $\boldsymbol{G}$. The elementary eigenstates would have equal probability:

$$p_i = {}^{1}\!/_{M} \quad \forall\ \boldsymbol{i} \in \boldsymbol{G} \tag{2}$$

, where M is the cardinality of set $\boldsymbol{G}$. I introduce functions $\mathcal{E},\ \mu$ as follows:

$$\ln P\big((n_i);\ N,(p_i)\big) = \mu\big(N,(p_i)\big) - \mathcal{E}\big((n_i);\ N,(p_i)\big) \tag{3}$$

$$\mu\big(N,(p_i)\big) = \ln P\big((n_i \equiv N\cdot p_i);\ N,(p_i)\big) = H_\Omega\big(N,(p_i)\big) - N\cdot H_S\big((p_i)\big) \tag{4}$$

$$H_\Omega\big(N,(p_i)\big) = H_\Omega(equilibrium) = \ln\Gamma(N+1) - \sum_{i\in\boldsymbol{G}} \ln\Gamma(Np_i+1) \tag{5}$$

$$\mathcal{E}\big((n_i);\ N,(p_i)\big) = \mu\big(N,(p_i)\big) - \ln P\big((n_i);\ N,(p_i)\big) = \sum_{i\in\boldsymbol{G}} \left[\ln\frac{\Gamma(n_i+1)}{\Gamma(Np_i+1)} + (Np_i - n_i)\cdot\ln p_i\right] \tag{6}$$

$$\mathcal{E}\big((n_i = Np_i \;\forall\; \boldsymbol{i} \in \boldsymbol{G});\; N, (p_i)\big) = 0 \tag{7}$$

, where $\Gamma(x)$ is *gamma* function; $$H_S\big((p_i)\big) = \big[H_\Omega\big(N, (p_i)\big)/N\big]_{N\to\infty} = -\sum_{i\in\boldsymbol{G}} p_i \ln p_i \tag{8}$$

Here $H_S\big((p_i)\big)$ is Shannon's [13] unit entropy, and $H_\Omega\big(N, (p_i)\big)$ is the entropy of *equilibrium*. With (4-6), I rewrite (1) as

$$P\big((n_i);\; N, (p_i)\big) = exp\left(\mu\big(N, (p_i)\big) - \mathcal{E}\big((n_i); N, (p_i)\big)\right) \tag{9}$$

From (9), the probability of an event sample $\{n_i\}$, among all samples of the same size N, is determined solely by the value of $\mathcal{E}\big((n_i); N, (p_i)\big)$. If I'm to use $\mathcal{E}$ as a single independent variable, I can write (9) in $\mathcal{E}$ domain as:

$$P\big(\mathcal{E}; N, (p_i)\big) = g\big(\mathcal{E}; N, (p_i)\big) \cdot exp\big(\mu\big(N, (p_i)\big) - \mathcal{E}\big) \tag{10}$$

Here $g\big(\mathcal{E}; N, (p_i)\big)$ is the multiplicity (degeneracy) of the given $\mathcal{E}$ value[1], i.e. a number of ways the same value of $\mathcal{E}$ is realized by different samples with given parameters $N, (p_i)$. There is no analytic expression for $g\big(\mathcal{E}; N, (p_i)\big)$, however, it is numerically computable. Table 1 contains $\mathcal{E}$, $g\big(\mathcal{E}; N, (p_i)\big)$ values calculated for several sets of parameters $N, (p_i)$. Figures 1-2 show distinct values of $\mathcal{E}$ in increasing order for several values of parameter N and probabilities (2) calculated from (6), using algorithm [14] for finding partitions $\{n_i\}$ of integer N into $\leq M$ parts [15]. The sum of $g\big(\mathcal{E}; N, (p_i)\big)$ over all distinct values of $\mathcal{E}$ is the total number of distinct samples. It is equal to the number of ways to distribute N indistinguishable balls into M distinguishable cells:

$$F(N, M) = \sum_{\{\mathcal{E}\}} g\big(\mathcal{E}; N, (p_i)\big) = \frac{(N + M - 1)!}{N!\,(M - 1)!} \tag{11}$$

, where sum is over all distinct values of $\mathcal{E}$. Figure 3 shows the total number $F(N, M)$ of distinct event samples, and the total number of distinct values $\{\mathcal{E}\}$ as functions of N for two sets of probabilities (2), calculated from (11) and (6) using algorithm [14]. The graphs demonstrate that:

- For probabilities (2), the average degeneracy of $\{\mathcal{E}\}$ levels $\langle g\rangle_{N\to\infty} = M!$

This statement can be expressed as:

$$M! \cdot \lim_{N\to\infty} \sum_{\{\mathcal{E}\}} 1 = \frac{(N + M - 1)!}{N!\,(M - 1)!} \tag{12}$$

Here $\sum_{\{\mathcal{E}\}} 1$ sum represents the number of distinct values of $\mathcal{E}$ for the given parameters N, M. $g\big(\mathcal{E}; N, (p_i)\big)$ can exceed $M!$ in some cases. E.g. $g\big(\mathcal{E} = 8.0731; N = 50, p_{\{i\}} = 1/3\big) = 12$ because $\mathcal{E}(\{n_i\} = \{29,15,6\}; 50,3) = \mathcal{E}(\{n_i\} = \{30,13,7\}; 50,3) = 8.0731$. Another example is, $\mathcal{E}(\{n_i\} = \{10,3,2\}; 15,3) = \mathcal{E}(\{n_i\} = \{9,5,1\}; 15,3) = 3.226844$.

As $g\big(\mathcal{E}; N, (p_i)\big)$ is not a smooth function of $\mathcal{E}$ (see Table 1), there could be no true probability density in $\mathcal{E}$ domain. I shall derive pseudo probability density to be used in expressions involving integration by $\mathcal{E}$ in *thermodynamic limit*. To be able to use analytical math, I have to extend (4-9) from discrete variables $\{n_i\}$ to continuous domain. I call

- *Thermodynamic limit* is the approximation of large occupation numbers:

$$n_i \gg 1 \;\forall\; \boldsymbol{i} \in \boldsymbol{G} \tag{13}$$

[1] In case of a sample with event probabilities (2); the multiplicity of $\mathcal{E}$ is the multiplicity of the value of multinomial coefficient in (1) [41]

In thermodynamic limit, I can use Stirling's approximation for factorials

$$\ln n! \approx \frac{1}{2}\ln 2\pi n + n\ln n - n \tag{14}$$

It allows rewriting of (4, 6), for probabilities (2), as

$$\mu\big(N,(p_i)\big) \cong -\frac{1}{2}\left[(M-1)\cdot\ln 2\pi N + \ln\prod_{i\in \boldsymbol{G}} p_i\right] \Rightarrow \mu(N,M) = \frac{M}{2}\ln M - \frac{M-1}{2}\ln 2\pi N \tag{15}$$

$$\mathcal{E}\big((n_i);\ N,(p_i)\big) \cong \sum_{i\in \boldsymbol{G}}\left(n_i+\frac{1}{2}\right)\cdot\ln\frac{n_i}{Np_i} = \sum_{i\in \boldsymbol{G}}\left(n_i+\frac{1}{2}\right)\cdot\ln n_i - \left(N+\frac{M}{2}\right)\ln\frac{N}{M} \tag{16}$$

Expr. (16) reverberates with the proposed [16] electron correlation energy $E_{cor} = \varkappa\sum n_i \ln n_i$. Figures 4,5 demonstrate functions $\mu\big(N,(p_i)\big)$ and $\mathcal{E}$ calculated for two sets of parameters (p_i) using exact expressions (4), (6), and approximations (15), (16).

In thermodynamic limit, $\mathcal{E}$ is a smooth function of $\{n_i\}$ approximated by positive semi-definite quadratic form of $\{n_i - Np_i\}$ in the vicinity of its minimum (7):

$$\mathcal{E} \cong \sum_{\substack{i\in \boldsymbol{G}\\ j\in \boldsymbol{G}}} b_{ij}\cdot(n_i - Np_i)\cdot\big(n_j - Np_j\big) \tag{17}$$

Knowing the covariance matrix [17] of multinomial distribution (1) allows reduction of (17) to diagonal form. The covariance matrix, divided by N is:

$$\sigma_{ij} = \delta_{ij}\cdot p_j - p_i\cdot p_j \qquad \text{, where} \qquad \delta_{i=j} = 1 \quad ;\ \delta_{i\neq j} = 0 \tag{18}$$

The rank of σ_{ij} is $M-1$. If d_{ij} is a diagonal form of σ_{ij}, the eigenvalues of σ_{ij} are $d_i = d_{ii}$:

$$d_{ij} = diag\big(\sigma_{ij}\big) \quad ; \quad d_i = d_{ii} \quad ; \quad d_1 \equiv 0 \quad ; \quad d_{i>1} > 0 \tag{19}$$

For equal probabilities (2), $d_{i>1} = 1/M$. I transform to new discrete variables:

$$x_{i>1} = \sum_{j\in \boldsymbol{G}}\big(n_j - Np_j\big)\frac{\Theta_{ji}}{\sqrt{d_i}} = \sqrt{M}\sum_{j\in \boldsymbol{G}}\left(n_j - \frac{N}{M}\right)\cdot\Theta_{ji} \qquad ; x_1 \equiv 0 \tag{20}$$

, where Θ_{ij} is matrix with columns as unit eigenvectors of σ_{ij} corresponding to eigenvalues (19). In case of $M = 3$ and probabilities (2)

$$\Theta_{ij} = \begin{bmatrix} 1/\sqrt{3} & -1/\sqrt{6} & 1/\sqrt{2} \\ 1/\sqrt{3} & -1/\sqrt{6} & -1/\sqrt{2} \\ 1/\sqrt{3} & \sqrt{2/3} & 0 \end{bmatrix} \tag{21}$$

The eigenvector Θ_{i1} corresponding to eigenvalue $d_1 \equiv 0$ is perpendicular to hyper-plane defined by $\sum_{i\in \boldsymbol{G}} n_i = N$ in M-dimensional space of $\{i \in \boldsymbol{G}\}$ coordinates, while vector $(n_i - Np_i)$ is parallel to the hyper-plane. Therefore, $x_1 \equiv 0$ in (20). I rewrite (17) in terms of new variables $\{x_i\}$ as:

$$\mathcal{E} = \frac{1}{2N}\sum_{i\in \boldsymbol{G}} x_i^2 = \frac{\langle \boldsymbol{x}|\boldsymbol{x}\rangle}{2N} = \frac{M}{2N}\sum_{i\in \boldsymbol{G}}\left(n_i - \frac{N}{M}\right)^2 \tag{22}$$

I call $\{x_i\}$ the *canonical variables* of the sample, and $\boldsymbol{x} = (x_i)$ the *canonical momentum*. I call parameter $\mathcal{E}$ the *energy*. N plays a role of *mass*. From (5, 6), for probabilities (2), it follows:

$$\mathcal{E}\big((n_i);\ N,(p_i)\big) = H_\Omega\big(N,(p_i)\big) - H_\Omega\big((n_i);\ N\big) \tag{23}$$

, where

$$H_\Omega\big((n_i);\ N\big) = \ln\Gamma(N+1) - \sum_{i\in \boldsymbol{G}} \ln\Gamma(n_i+1) \tag{24}$$

Hence, for elementary eigenstates, energy equals difference between entropy $H_\Omega\big(N,(p_i)\big)$ of equilibrium, and entropy $H_\Omega(\{n_i\};\ N)$ of the sample, i.e. energy equals *knowledge* [about object state]. As entropies (5), (24) are in units of *nats*, so is the energy (6,16,22,23).

Figure 5 demonstrates function $\sqrt{\mathcal{E}/N}$ calculated for two sets of parameters (p_i) using exact expression (6) and approximations (16), and (22). I plotted $\sqrt{\mathcal{E}/N}$ instead of $\mathcal{E}$ to show asymptotic behavior of (6) and (16) in comparison with quadratic form (22). Using (9, 15, 22) I obtain multivariate normal approximation [17] to multinomial distribution (1) as

$$P\big((x_i);\ N,(p_i)\big) \cong (2\pi N)^{\frac{1-M}{2}} \cdot exp\left[-\sum_{i\in \boldsymbol{G}}\left(\frac{x_i^2}{2N} + \frac{\ln p_i}{2}\right)\right] = exp\left[\mu\big(N,(p_i)\big) - \sum_{i\in \boldsymbol{G}}\frac{x_i^2}{2N}\right] \tag{25}$$

Figure 6 shows graphs of $\ln P\big((n_i);N,(p_i)\big)$ as a function of n_1 calculated for $N = 1000$ and four sets of probabilities (p_i), using exact formula (1), and multivariate normal approximation (25).

In order to derive pseudo probability density in $\mathcal{E}$ domain, I note that:

- In thermodynamic limit, the number $F(\mathcal{E}_0;N,M)$ of distinct event samples having $\mathcal{E} \le \mathcal{E}_0$ is proportional to the volume of $(M-1)$ –dimensional sphere of radius $|\boldsymbol{x}_0| = \sqrt{2N\mathcal{E}_0}$. This statement can be expressed as

$$F(\mathcal{E}_0;N,M) = \lim_{N\to\infty}\sum_{\{\mathcal{E}\}\le\mathcal{E}_0} g(\mathcal{E};N,M) = a(N,M)\cdot(2N\mathcal{E}_0)^{\frac{M-1}{2}} \tag{26}$$

The sum in (26) is over all distinct values of $\mathcal{E}$ which are less or equal than $\mathcal{E}_0$. The function $a(N,M)$ is determined from normalization requirement:

$$1 = \sum_{\{\mathcal{E}\}} P(\mathcal{E};N,M) = \sum_{\{\mathcal{E}\}} g(\mathcal{E};N,M)\cdot exp(\mu(N,M)-\mathcal{E}) \tag{27}$$

In order to convert from sums to integrals over continuous variable $\mathcal{E}$, I define pseudo density $g(\mathcal{E};N,M)$ of object states as

$$g(\mathcal{E};N,M) = \frac{\partial}{\partial\mathcal{E}}F(\mathcal{E};N,M) = a(N,M)\cdot\frac{M-1}{2}\cdot(2N)^{\frac{M-1}{2}}\cdot\mathcal{E}^{\frac{M-3}{2}} \tag{28}$$

The corresponding pseudo probability density $P(\mathcal{E};N,M)$ is given by (10). The normalization requirement for these functions becomes:

$$1 = \int_0^{\mathcal{E}_{max}} P(\mathcal{E};N,M)d\mathcal{E} = \int_0^{\mathcal{E}_{max}} g(\mathcal{E};N,M)\cdot exp(\mu(N,M)-\mathcal{E})d\mathcal{E} \tag{29}$$

The $\mathcal{E}_{max}$ value is obtained from (6) by having event $\boldsymbol{j}$ with lowest probability $p_{min} = \min_{\boldsymbol{i}\in\boldsymbol{G}}\{p_i\}$ acquire maximum population: $n_{\boldsymbol{j}} = N;\ n_{i\neq j} = 0$. From (6), as $N\to\infty$:

$$\mathcal{E}_{max}\big(N,(p_i)\big) \cong -N\cdot\ln p_{min} \tag{30}$$

For probabilities (2):

$$\mathcal{E}_{max}(N,M) \cong N\cdot\ln M - \frac{M-1}{2}\ln 2\pi N + \frac{M}{2}\ln M \tag{31}$$

From (31) $\mathcal{E}_{max} \to \infty$ as $N \to \infty$. That allows replacing $\mathcal{E}_{max}$ in the upper limit of integral in (29) with ∞. The expression for function $a(N,M)$ in (26) is [17]:

$$a(N,M) = \left[e^{\mu(N,M)} \cdot (2N)^{\frac{M-1}{2}} \cdot \int_0^{\infty} \mathcal{E}^{\frac{M-1}{2}} e^{-\mathcal{E}} d\mathcal{E} \right]^{-1} = \frac{e^{-\mu(N,M)}}{(2N)^{\frac{M-1}{2}} \Gamma\left(\frac{M+1}{2}\right)} \tag{32}$$

Using (32, 15) I write (26) as

$$F(\mathcal{E};N,M) = \frac{\mathcal{E}^{\frac{M-1}{2}}}{\Gamma\left(\frac{M+1}{2}\right)} e^{-\mu(N,M)} = \frac{(2\pi N\mathcal{E})^{\frac{M-1}{2}}}{M^{\frac{M}{2}} \cdot \Gamma\left(\frac{M+1}{2}\right)} = \frac{V\left(\sqrt{2N\mathcal{E}}; M-1\right)}{M^{\frac{M}{2}}} \tag{33}$$

, where $V\left(\sqrt{2N\mathcal{E}}; M-1\right) = \frac{(2\pi N\mathcal{E})^{\frac{M-1}{2}}}{\Gamma\left(\frac{M+1}{2}\right)}$ is the volume of $(M-1)$ –dimensional sphere of radius $|\boldsymbol{x}| = \sqrt{2N\mathcal{E}}$.

The number $n(\mathcal{E})$ of distinct values of $\mathcal{E}$ in $N \to \infty$ limit can be estimated from (33, 12) as

$$n(\mathcal{E}) = \frac{F(\mathcal{E};N,M)}{M!} = \frac{(2\pi N\mathcal{E})^{\frac{M-1}{2}}}{M^{\frac{M}{2}} \cdot \Gamma\left(\frac{M+1}{2}\right) \Gamma(M+1)} \tag{34}$$

From (34), I can approximately enumerate distinct energy levels $\mathcal{E}_n$ by "quantum number" n:

$$\mathcal{E}_n = \left[\Gamma\left(\frac{M+1}{2}\right) \Gamma(M+1) e^{\mu(N,M)} \cdot n \right]^{\frac{2}{M-1}} = \frac{M}{2\pi N} \left[\Gamma\left(\frac{M+1}{2}\right) \Gamma(M+1) M^{\frac{1}{2}} \cdot n \right]^{\frac{2}{M-1}} \tag{35}$$

From (28, 33) the pseudo density $g(\mathcal{E};N,M)$ of object states is:

$$g(\mathcal{E};N,M) = \frac{\partial}{\partial \mathcal{E}} F(\mathcal{E};N,M) = \frac{\mathcal{E}^{\frac{M-3}{2}} e^{-\mu(N,M)}}{\Gamma\left(\frac{M-1}{2}\right)} \tag{36}$$

I use condition (11) to define effective $\mathcal{E}_{max}^{eff}$ value:

$$F(N,M) = F\left(\mathcal{E}_{max}^{eff}; N, M\right) = \frac{\mathcal{E}_{max}^{eff\ \frac{M-1}{2}}}{\Gamma\left(\frac{M+1}{2}\right)} e^{-\mu(N,M)} = \frac{(N+M-1)!}{N!\,(M-1)!} \tag{37}$$

Figure 7 shows $F(\mathcal{E};N,\{p_i\})$ calculated from expressions (1, 6), and from formula (33). From (10, 15, 36), the pseudo probability density function (*pdf*) of event samples in thermodynamic limit is

$$P(\mathcal{E};N,M) = \frac{\mathcal{E}^{\frac{M-3}{2}} e^{-\mathcal{E}}}{\Gamma\left(\frac{M-1}{2}\right)} = \gamma_{b,c}(\mathcal{E}); \qquad b = 1;\ \ c = \frac{M-1}{2} \tag{38}$$

, where $\gamma_{b,c}(\mathcal{E})$ is the *pdf* of *gamma* [17] distribution with scale parameter $b = 1$, and shape parameter $c = (M-1)/2$. I calculate moments of $\mathcal{E}$ in equilibrium:

Mean: $$\langle \mathcal{E} \rangle^{eq} = \sum_{\{n_i\}} \mathcal{E}\left((n_i);\ N,M\right) \cdot P\left((n_i);\ N,M\right) \tag{39}$$

Variance: $$\sigma_{\mathcal{E}}^2 = \sum_{\{n_i\}} \big(\mathcal{E}\big((n_i); N, M\big) - \langle\mathcal{E}\rangle\big)^2 \cdot P\big((n_i); N, M\big) \tag{40}$$

r^{th} moment about mean: $$\kappa_r(N, M) = \sum_{\{n_i\}} \big(\mathcal{E}\big((n_i);\ N, M\big) - \langle\mathcal{E}\rangle\big)^r \cdot P\big((n_i);\ N, M\big) \tag{41}$$

The sums in (39-41) are over all partitions of N. Expression (38) allows explicit calculation of all moments of $\mathcal{E}$ in thermodynamic limit. From (38) the mean value $\langle\mathcal{E}\rangle^{eq}$, the variance $\sigma_{\mathcal{E}}^2$, and the third moment κ_3, in equilibrium, are:

$$\langle\mathcal{E}\rangle^{eq} = \frac{M-1}{2} \tag{42}$$

$$\sigma_{\mathcal{E}}^2 = \frac{M-1}{2} \tag{43}$$

$$\kappa_3 = M - 1 \tag{44}$$

Figure 8 shows calculations of $\langle\mathcal{E}\rangle^{eq}$, $\sigma_{\mathcal{E}}^2$, and κ_3 from expressions (39-41) for the moments, with probability mass function (1). It demonstrates how these values asymptotically approach thermodynamic limit values (42-44) as $N \cdot p_i \to \infty$.

The knowledge about object's state is not full if sample size N is finite [13]. Even in case of maximum knowledge, when the sample of size N consists of the same event, there is $e^{-1}/(N+1)$ probability a sample of size $N+1$ will return two distinct events. I define *knowledge confidence* Λ as:

$$\Lambda = \frac{\mathcal{E}\big((n_i);\ N, (p_i)\big)}{N}\left[\frac{N}{\mathcal{E}_{max}\big(N, (p_i)\big)}\right]_{N\to\infty} = \frac{\mathcal{E}\big((n_i);\ N, (p_i)\big)}{N \ln M} \tag{45}$$

To illustrate the notion of knowledge confidence, imagine an experiment to determine polarization of a light source with a polarizer coupled to light detector. If all N photons from the source arrive at the detector, does it mean I know the polarization of light source with absolute certainty? The answer is no, since there is a chance, if I repeat the experiment with $N+1$ photons, at least one photon will be lost in polarizer.

I shall demonstrate how the presented model correlates with some known constructs. Consider one-dimensional quantum harmonic oscillator. Its energy levels [18] are given by:

$$\mathcal{E}_n = \left(n + \frac{1}{2}\right) \cdot \Delta\mathcal{E} \tag{46}$$

, where $\Delta\mathcal{E}$ is the interval between energy levels; n = 0,1,2 ... . Energy levels (46) are equally-spaced. The energy levels of event sample of cardinality $M = 3$ exhibit similar pattern. As shown on Figure 1, linear dependence on quantum number n holds reasonably well if n is not too large. From (12), the linearity breaks down when $n \geq N^2/24$. From (22):

$$\mathcal{E} = \sum_{i\in\boldsymbol{G}} \frac{{\Delta_i}^2}{2 \cdot \langle n\rangle} \tag{47}$$

, where $$\Delta_i = n_i - \langle n\rangle \quad ; \quad \sum_i \Delta_i = 0 \quad ; \quad \langle n\rangle = \frac{N}{M} \tag{48}$$

From above, the energy levels of an event sample of cardinality $M = 3$ are:

$$\mathcal{E}_k = \frac{L_k}{N} \tag{49}$$

, where L_k are *Loeschian numbers* [19]. With (46, 49), I can write the comparison table of the first few energy levels of quantum harmonic oscillator in units of $\Delta\mathcal{E}/2$, and of event sample of cardinality $M = 3$ in units $1/N$:

quantum harmonic oscillator		1	3		5	7	9	11		13	15		17	19	21	23	25	27		29	31	33	35		37	39	41	43
event sample of cardinality $M = 3$	0	1	3	4		7	9		12	13		16		19	21		25	27	28		31			36	37	39		43

, where black boxes designate missing energy levels. In the second row, the energy levels shown in shaded boxes are only realized for samples with sizes satisfying $mod(N, 3) > 0$; and energy levels shown in white boxes are realized for samples with sizes satisfying $mod(N, 3) = 0$. Here $mod(N, 3)$ is the remainder of division of N by 3.

Consider another quantum mechanical example: particle of mass m in a box of size L. Its energy levels [18] are given by:

$$\mathcal{E}_n = \frac{h^2}{8mL^2} n^2 \quad ; \quad n = 1,2,3 \ldots \tag{50}$$

In presented model, similar energy spectrum is exhibited by event sample of cardinality $M = 2$, as shown on Figure 2. From (47), the energy levels of an event sample of cardinality $M = 2$, in thermodynamic limit approximation, are:

$$\mathcal{E}_n = \frac{n^2}{2N} = \frac{h^2}{8mL^2} n^2 \quad ; \quad n = 0,1,2 \ldots \tag{51}$$

, where $m = N \cdot \left(\frac{h}{2L}\right)^2$ is to be considered as the *effective mass* of the particle. (52)

Energy levels (51) with even n are only possible when N is even, and energy levels with odd n are only possible when N is odd. With ½ probability the lowest energy level is $\mathcal{E} = \mathcal{E}_0 = 0$, and with ½ probability it is $\mathcal{E} = \mathcal{E}_1 = 1$, in units of $h^2/(8mL^2)$.

3. THERMODYNAMIC ENSEMBLE

In previous section, the event sample represented a single object. In this section I consider a collection of objects; each object represented by an event sample of size N, and cardinality M. I call such collection *thermodynamic ensemble*. Objects with different N or M belong to different thermodynamic ensembles. I call event sample $\{n_i\}$ a *mode*. I designate $\{\boldsymbol{k}\}$ the set of *modes* an object may occupy, and $K_{\boldsymbol{k}}$ the number of objects in mode $\boldsymbol{k}$:

$$\sum_{\{\boldsymbol{k}\}} K_{\boldsymbol{k}} = K \tag{53}$$

The probability for an object to be in mode $\boldsymbol{k}$ is given by (1, 9). Objects in the same mode $\boldsymbol{k}$ are indistinguishable, by definition of measurement. The probability mass function of distribution of modes among objects is:

$$P\big((K_{\boldsymbol{k}});\ K, (p_{\boldsymbol{k}})\big) = K! \prod_{\{\boldsymbol{k}\}} \frac{p_{\boldsymbol{k}}^{K_{\boldsymbol{k}}}}{K_{\boldsymbol{k}}!} \tag{54}$$

The objective is to find *equilibrium*, i.e. the most probable distribution (K_k). For a standalone object, the most probable distribution is the one which maximizes (54):

$$K_{\boldsymbol{k}} = K \cdot p_{\boldsymbol{k}} \tag{55}$$

Consider objects to be part of thermodynamic ensemble in a certain state. That imposes conditions on distribution of modes, so relations (42-44), (55) may no longer hold. I consider one of the possible conditions and show how it leads to the notion of *temperature*. Let the state of

thermodynamic ensemble be such that the mean energy of objects in equilibrium is $\langle\mathcal{E}\rangle^{eq}$, which may be different from equilibrium mean energy of a standalone object (42). Then:

$$\langle\mathcal{E}\rangle^{eq} \cdot K = \sum_{\{\boldsymbol{k}\}} K_{\boldsymbol{k}} \cdot \mathcal{E}_{\boldsymbol{k}} \tag{56}$$

To find the most probable distribution of modes $(K_{\boldsymbol{k}})$, I shall maximize logarithm of (54) using method of Lagrange multipliers [20] with conditions (53, 56):

$$\begin{aligned} \ln P\big((K_{\boldsymbol{k}});\, K, (p_{\boldsymbol{k}})\big) &= \ln\Gamma(K+1) + \sum_{\{\boldsymbol{k}\}} [K_{\boldsymbol{k}} \cdot \ln p_{\boldsymbol{k}} - \ln\Gamma(K_{\boldsymbol{k}}+1)] \\ &= \ln\Gamma(K+1) + \sum_{\{\boldsymbol{k}\}} [K_{\boldsymbol{k}} \cdot (\mu - \mathcal{E}_{\boldsymbol{k}}) - \ln\Gamma(K_{\boldsymbol{k}}+1)] \end{aligned} \tag{57}$$

From (57, 56, 53) I obtain the following equation involving Lagrange multipliers α and β:

$$\Psi_0(K_{\boldsymbol{k}}+1) = \mu - (1+\alpha)\cdot\mathcal{E}_{\boldsymbol{k}} - \beta \tag{58}$$

, where Ψ_0 is *digamma* function, and α and β are to be determined by solving (58) for $K_{\boldsymbol{k}}$:

$$K_{\boldsymbol{k}} = \Psi_0^{-1}\left(\mu - \frac{\mathcal{E}_{\boldsymbol{k}}}{T} - \beta\right) - 1 \tag{59}$$

, and by plugging $K_{\boldsymbol{k}}$ from (59) into (56) and (53). In (59), Ψ_0^{-1} is the inverse digamma function, and $1/T = 1 + \alpha$. The parameter T is commonly known as *temperature*.

Since the number of objects $K_{\boldsymbol{k}}$ in mode $\boldsymbol{k}$ cannot be negative, expression (59) effectively limits modes which can be present in equilibrium to those satisfying

$$\mu - \frac{\mathcal{E}_{\boldsymbol{k}}}{T} - \beta + \gamma \geq 0 \tag{60}$$

, where $\gamma \cong 0.577215665$ is *Euler–Mascheroni* constant. With approximation [21]: $exp\big(\Psi_0(K_{\boldsymbol{k}}+1)\big) \cong K_{\boldsymbol{k}} + 1/2$; I rewrite (59) as:

$$K_{\boldsymbol{k}} \cong exp\left(\mu - \frac{\mathcal{E}_{\boldsymbol{k}}}{T} - \beta\right) - \frac{1}{2} \tag{61}$$

Presence of $-½$ term in (61) leads to a computationally horrendous task of calculating β and T, because the summation in (53, 56) has to be only performed for modes satisfying (60). I shall leave the exact computation to a separate exercise, and make a shortcut, by ignoring $-½$ term in (61). This approximation is equivalent to Boltzmann's postulate[2] that the number of objects in mode $\boldsymbol{k}$, in equilibrium, is proportional to $exp(-\mathcal{E}_{\boldsymbol{k}}/T)$. The shortcut allows calculation of Lagrange multiplier β from (53):

$$exp(-\beta) = \frac{K}{Z(T)} \quad \text{, where} \quad Z(T) = \sum_{\{\boldsymbol{k}\}} exp\left(\mu - \frac{\mathcal{E}_{\boldsymbol{k}}}{T}\right) \tag{62}$$

Using (36), the partition function $Z(T)$ in (62) can be evaluated as:

$$Z(T) = \sum_{\{\boldsymbol{k}\}} exp\left(\mu - \frac{\mathcal{E}_{\boldsymbol{k}}}{T}\right) = \int_0^\infty \frac{\mathcal{E}^{\frac{M-3}{2}}}{\Gamma\left(\frac{M-1}{2}\right)} exp\left(-\frac{\mathcal{E}}{T}\right) d\mathcal{E} = T^{\frac{M-1}{2}} \tag{63}$$

The equation (56) then becomes

$$\langle\mathcal{E}\rangle^{eq} = T^2 \cdot \frac{\partial}{T} \ln Z = \frac{M-1}{2} \cdot T \tag{64}$$

[2] While widely used, this postulate has rather unphysical consequence that there is a non-zero probability of finding an object in a mode with arbitrary large energy. Another consequence is the divergence of partition function for some constructs, e.g. hydrogen electronic levels [40].

Eq. (64) is the relation [22] between mean per-particle energy and temperature in $(M-1)$-dimensional Maxwell-Boltzmann gas.

The *thermodynamic equilibrium per-object entropy* H_T^{eq} is the number of *nats* required to encode distribution of modes in equilibrium. Using (15) and (64), I evaluate H_T^{eq} in $K \to \infty$ limit:

$$\mathrm{H}_T^{eq} = -\sum_{\{\boldsymbol{k}\}} p_{\boldsymbol{k}} \cdot \ln p_{\boldsymbol{k}} = \frac{M-1}{2}\ln(eT) - \mu \cong \frac{M-1}{2}\ln(2\pi eN \cdot T) - \frac{M}{2}\ln M \tag{65}$$

, where

$$p_{\boldsymbol{k}} = exp\left(\mu - \frac{\mathcal{E}_{\boldsymbol{k}}}{T}\right)/Z(T) \tag{66}$$

In case of $M = 4$, i.e. for $(M-1) = 3$ degrees of freedom, expression (65) turns into equivalent of Sackur-Tetrode equation [22] for the entropy of ideal gas. For thermodynamic equilibrium entropy of a standalone object, instead of (65), I have:

$$\mathrm{H}^{eq} = \langle\mathcal{E}\rangle^{eq} - \mu = \frac{M-1}{2}\ln(2\pi eN) - \frac{M}{2}\ln M \tag{67}$$

The difference of entropies (65, 67) by $\frac{M-1}{2}\ln T$ term is due to spread in object energies. The non-zero thermodynamic entropy means the mode is unknown prior to observation, for each observation. I rewrite (67) as:

$$\mathrm{H}^{eq} = \mathrm{H}_0^{eq}(M) + \frac{M-1}{2}\ln N \quad ; \text{where} \quad \mathrm{H}_0^{eq}(M) = \frac{M-1}{2}\ln 2\pi e - \frac{M}{2}\ln M \tag{68}$$

The expression for $\mathrm{H}_0^{eq}(M)$ in (68) was derived in thermodynamic limit, i.e. when $N \to \infty$. When $N = 1$, $\mathrm{H}^{eq} = \ln M$. By comparing $\mathrm{H}_0^{eq}(M)$ to $\ln M$ (Figure 9) I see that $\mathrm{H}_0^{eq}(M)$ fairly close to $\ln M$ except when M is large enough, in which case thermodynamic limit approximation for the given N becomes less valid anyhow. Therefore, I can replace $\mathrm{H}_0^{eq}(M)$ with $\ln M$ in (68) and write thermodynamic equilibrium entropy as:

$$\mathrm{H}^{eq} = \ln M + \frac{M-1}{2}\ln N \quad ; \quad \mathrm{H}_T^{eq} = \ln M + \frac{M-1}{2}\ln(NT) \tag{69}$$

Figure 10 shows the comparison of thermodynamic equilibrium entropy H^{eq} of a standalone object in $K \to \infty$ limit, calculated from $\mathrm{H}^{eq} = -\sum_{\{\boldsymbol{k}\}} p_{\boldsymbol{k}} \cdot \ln p_{\boldsymbol{k}}$, and from (69). Since H_T^{eq} should be $\geq \ln M$, it means T cannot be less than $1/N$.

The expression for $Z(T)$ in (63) has been derived in thermodynamic limit approximation, i.e. when $N \to \infty$. It means there must be large number of energy levels included in sum (63), i.e. temperature T cannot be too small. Therefore, the expressions (63-64) are only valid for $T \gg \Delta\mathcal{E}$, where $\Delta\mathcal{E}$ is the characteristic difference between adjacent energy levels.

For an event sample of cardinality $M = 3$ the approximately evenly-spaced energy levels (Figure 1) allow for more accurate expression for partition function. From (35) the characteristic difference between adjacent energy levels is:

$$\langle\Delta\mathcal{E}\rangle = \frac{M!}{g(\mathcal{E}; N, M)} = 6 \cdot exp(\mu) = \frac{18\sqrt{3}}{2\pi N} \cong \frac{5}{N} \tag{70}$$

Figure 11 shows the numeric calculation of the difference $\Delta\mathcal{E}$ between adjacent energy levels averaged over distinct event samples with the given value of N, and $M = 3$. I can use (46), with degeneracy of each level g=6, as an approximation for combined energy levels (49) in expression for partition function (63), and obtain mean energy of modes with given N as [23]:

$$\langle \mathcal{E} \rangle^{eq} = \frac{\Delta\mathcal{E}}{2} + \frac{\Delta\mathcal{E}}{\exp\left(\frac{\Delta\mathcal{E}}{T}\right) - 1} \qquad ; \ \Delta\mathcal{E} = 2/N \tag{71}$$

Eq. (71) reduces to (64) if $T \gg \Delta\mathcal{E}$. (71) has been derived using linear dependence (46) of energy levels $\mathcal{E}_n$ on *quantum number* n, in $N \gg 1$, i.e. $\Delta\mathcal{E} \ll 1$ limit. For a black-body spectrum, the $\Delta\mathcal{E} \ll 1$ condition for validity of (71) has to be satisfied for $\Delta\mathcal{E} > T$ as well. Therefore, a typical black-body spectrum can only be exhibited by ensembles with $1/N < T < 5/N$; $N \gg 1$. An example is cosmic microwave background. The higher the temperature, the less accurate (71) will be in $\Delta\mathcal{E} > T$ region, where spectral intensity would fall off steeper than in (71). Such deviation from black-body is obvious in solar spectrum.

The zero-point energy term $\Delta\mathcal{E}/2$ in (71) is the subject of a hundred-year controversy [24, 25]. The conventional theory views radiation as existing "out there", decoupled from the matter. Such view leads to the infinite energy density due to the infinite number of hypothetically possible decoupled radiation modes, each multiplied by $\hbar\omega/2$ [23]. The conventional theory has no upper limit on $\hbar\omega$, short of an artificial cut-off, usually assumed at Planck energy. Even with frequency cut-off, there is still a discrepancy with empirical evidence of at least 58 orders of magnitude [25], possibly the biggest contradiction of any theory. In presented model, $\Delta\mathcal{E}/2$ term cannot contribute more than $(1/N) \ll 1$ to average energy, i.e. its contribution is well within standard deviation.

Thermodynamic ensemble is the statistical ensemble of non-elementary eigenstates whose probabilities $\{p_{\boldsymbol{k}}\}$ are given by (66), as opposed to elementary eigenstates' probabilities given by (2). Using (66, 5, 24) in formula (6) for energy of arbitrary non-equilibrium state, and substituting $\boldsymbol{k}$ for $\boldsymbol{i}$, K for N, and $K_{\boldsymbol{k}}$ for $n_{\boldsymbol{i}}$:

$$E_T = H_\Omega^{eq} - H_\Omega + \sum_{\{\boldsymbol{k}\}} K_{\boldsymbol{k}} \cdot [\mathcal{E}_{\boldsymbol{k}} - \langle \mathcal{E} \rangle^{eq}]/T = H_\Omega^{eq} - H_\Omega + K \cdot [\langle \mathcal{E} \rangle - \langle \mathcal{E} \rangle^{eq}]/T \tag{72}$$

Here H_Ω^{eq} is the entropy (5) of the ensemble, and $\langle \mathcal{E} \rangle^{eq}$ is objects' mean energy, in equilibrium. I rewrite (72) in terms of per-object quantities $\mathcal{E}_T = E_T/K$; $\mathrm{H}_T = H_\Omega/K$, in the limit $K \to \infty$:

$$T \cdot \mathcal{E}_T = T \cdot \left(\mathrm{H}_T^{eq} - \mathrm{H}_T\right) + \langle \mathcal{E} \rangle - \langle \mathcal{E} \rangle^{eq} = -T\Delta\mathrm{H} + \Delta U = \Delta W \tag{73}$$

Here $\Delta U = \langle \mathcal{E} \rangle - \langle \mathcal{E} \rangle^{eq}$; $\Delta\mathrm{H} = \mathrm{H}_T - \mathrm{H}_T^{eq}$ is the deviation of objects' mean *internal energy*, and of mean thermodynamic entropy, from their equilibrium values; $\Delta W = T \cdot \mathcal{E}_T$ is the *work* done on ensemble. As expected, from (73), $\mathcal{E}_T^{eq} = 0$. Eq. (73) represents the First Law of Thermodynamics. For ensemble of non-elementary eigenstates, $H_\Omega^{eq} \leq H_\Omega^{max}$, where H_Ω^{max} is the maximum entropy, achieved with equal population numbers $\{K_{\boldsymbol{k}}\}$ in (54). It means, in thermodynamic ensemble, according to (72, 73), part of the knowledge is associated with objects' internal energy.

4. THE MEASUREMENT

Measurement is one of the most debated topics in conventional theory [26, 27]. The controversy is stirred by the discreteness of outcomes of the measurement on quantum objects. A concept of wave function collapse has been devised early on, more as illustration, than explanation. The collapse concept is an awkward amalgamation of quantum postulate [28], and an implicit assumption of wave function's physical reality (PR). The collapse concept is prevalent [29] despite its contradiction with other accepted frameworks, such as special relativity. A burlesque scenario can be imagined: using wave function of a photon, which has to be non-zero everywhere up to the moment of measurement, one can instantly communicate with an observer on the opposite side of the galaxy, by absorbing photons coming from a star near the center of galaxy, and thus impacting probability of the same photons being detected by the remote observer. A similar scenario inspired

EPR paradox [30]. To work around the problem, a number of alternative QM interpretations, such as many-world [31], and pilot wave [32], have been proposed, still maintaining the PR viewpoint.

The measurement problem disappears if we stop attributing PR to wave function, and stop mistaking correlation for causality. In this section I show the concept of wave function is superfluous, and that treating measurement as *event sampling* is consistent with predictions of conventional QM, without its controversial baggage. I discuss the basics of conventional QM: wave function, Born rule, and Schrödinger equation, emphasizing their true meaning which is rarely, if ever, mentioned in textbooks. I derive similar expressions using event sample as base construct, demonstrating the connection between QM and the presented model. I explain the mechanics of observation, and the role of observer. I show how model extends to include transition from quantum to classical state, dispersion and decoherence.

The following experiment illustrates the delusion of wave function collapse concept, and of EPR "paradox": put a pair of gloves (left-hand and right-hand) randomly into two boxes, and let Alice and Bob each pick a box. Until one of them opens a box, no one knows who has which glove. To the same effect, the pair of gloves can be substituted by a pair of entangled particles having opposite spin, in a gedankenexperiment. The conventional QM describes situation as superposition

$$\psi_1 = \left[\pm Alice_{left} \otimes Bob_{right} \mp Alice_{right} \otimes Bob_{left}\right]/\sqrt{2} \tag{74}$$

, where $\pm$ signs enforce parity flip if Alice and Bob swap boxes, since mirror image of a left-hand glove is a right-hand glove. The lower sign corresponds to mirror image. If Alice finds left-hand glove in her box, Bob would find right-hand glove in his. In this case, conventional theory says, the wave function (74) collapsed into $\boldsymbol{k}_1 = Alice_{left} \otimes Bob_{right}$ eigenstate. Has Alice finding left-hand glove caused collapse of ψ_1, and, as a result, Bob to find right-hand glove in his box? Of course not. That is correlation, not causality, just like EPR case, where authors considered a pair of entangled particles. The distinct outcomes of the measurement (the event sample) are determined by the observation basis. A sampled event is one of object's eigenstates in a given observation basis. In example above, the object consists of two particles: two glove boxes, entangled by glove pairing. Each particle produces event sample of cardinality $M = 2$ (left or right glove). The events produced by different particles are correlated due to entanglement between the particles, even though events in each particle basis are completely random. The object's eigenstates are composed as direct product of particle eigenstates. The state (74) is one of object's eigenstates in *preparation* basis. The other 3 eigenstates could be constructed as:

$$\psi_2 = \left[Alice_{left} \otimes Bob_{right} + Alice_{right} \otimes Bob_{left}\right]/\sqrt{2}$$
$$\psi_3 = \left[\pm Alice_{left} \otimes Bob_{left} \mp Alice_{right} \otimes Bob_{right}\right]/\sqrt{2}$$
$$\psi_4 = \left[Alice_{left} \otimes Bob_{left} + Alice_{right} \otimes Bob_{right}\right]/\sqrt{2}$$

In the *measurement* basis, the object's eigenstates are:

$$\boldsymbol{k}_1 = Alice_{left} \otimes Bob_{right}$$
$$\boldsymbol{k}_2 = Alice_{right} \otimes Bob_{left}$$
$$\boldsymbol{k}_3 = Alice_{left} \otimes Bob_{left}$$
$$\boldsymbol{k}_4 = Alice_{right} \otimes Bob_{right}$$

There are two observation bases involved in determining the conditional probability of finding object in state $\boldsymbol{k}$, given it was prepared in state ψ. The observation bases are usually related by a [macroscopic parameter]-driven unitary transformation, albeit there are examples from quantum field theory (QFT), when they are not [33]. There could be no unitary transformation between observation bases of different cardinality M. In example, the observation bases of *preparation* and of *measurement* are rotated with respect to each other by $\pi/4$ within plane formed by vectors

$\boldsymbol{k}_1, \boldsymbol{k}_2$. The observation basis rotated when boxes became identifiable (i.e. separated) by a parameter (distance): one box got to Alice and another box to Bob. This is an example of a unitary transformation of observation basis with distance as transformation parameter.

At the core of conventional QM lies Born rule. It stipulates the probability $\wp_{\boldsymbol{k}}$ of a particular outcome $\boldsymbol{k}$ of a measurement performed on state [vector] ψ is

$$\wp_{\boldsymbol{k}} = \frac{|\langle\psi|\boldsymbol{k}\rangle|^2}{\langle\psi|\psi\rangle\langle\boldsymbol{k}|\boldsymbol{k}\rangle} = \cos^2\varphi_{\psi,\boldsymbol{k}} \tag{75}$$

, where $\varphi_{\psi,\boldsymbol{k}}$ is the angle between ψ and $\boldsymbol{k}$. If vectors $\{\boldsymbol{k}\} \in \boldsymbol{G}$ constitute an eigenbasis, then

$$\sum_{\boldsymbol{k}} \wp_{\boldsymbol{k}} = 1 \tag{76}$$

The rest of QM deals with how probabilities (75) change with parameter-driven unitary transformation of eigenbasis $\{\boldsymbol{k}\}$. The Born rule is a *conditional probability*, i.e. a probability of outcome $\boldsymbol{k}$, given the object was prepared in state ψ. In example above, the conditional probability of outcomes $\boldsymbol{k}_1$ ... $\boldsymbol{k}_4$, given preparation (74) are:

$$\wp_1 = \frac{1}{2}\ ;\ \wp_2 = \frac{1}{2}\ ;\ \wp_3 = 0\ ;\ \wp_4 = 0$$

Conventional QM does not deal with unconditional probabilities. QM predicts results of a measurement, if the state of an object is already known in some observation basis. The conditional measurement requires two or more particles to be entangled via some medium [23]. The entanglement enforces correlation between object's eigenstates in preparation and measurement bases. That is the underlying setting, albeit not widely acknowledged, for Born rule.

For any state ψ there exists an observation basis in which ψ has only one non-zero eigenstate component:

$$|\psi\rangle = \boldsymbol{U}^{\dagger}|0\ldots, n_{\boldsymbol{k}} = N, 0\ldots\rangle \tag{77}$$

, where $\boldsymbol{U}$ is a unitary transformation to eigenbasis in which $|\psi\rangle = |0\ldots, N, 0\ldots\rangle$. It corresponds to a situation when all N measurement events are a particular outcome $\boldsymbol{k}$, as e.g. detection of polarized photons using polarizer aligned with photon polarization.

Schrödinger equation, in its true meaning, describes a parameter-driven unitary transformation of observation basis. The usual parameter of transformation is *time*, but it can be other parameter, e.g. *distance*. The integral form of Schrödinger equation:

$$\psi(t) = \boldsymbol{U}^{\dagger}(t; t_0)\cdot\psi(t_0) = \ exp\left[-i\int_{t_0}^{t}\partial t\cdot\boldsymbol{\mathcal{H}}\right]\cdot\psi(t_0) \tag{78}$$

is the same equation as (77), where $\boldsymbol{U}$ is a unitary transform generated by Hermitian operator $\boldsymbol{\mathcal{H}}$. From (77), the eigenbasis components of quantum state must have certain phase relations with each other, enforced by $\boldsymbol{U}$. In case of a time-driven unitary transformation (78), generated by time-independent $\boldsymbol{\mathcal{H}}$, the phase relations between $\boldsymbol{k}$ and $\boldsymbol{j}$ eigenvector components are:

$$\varphi_{\boldsymbol{k}} - \varphi_{\boldsymbol{j}} = \left(E_{\boldsymbol{k}} - E_{\boldsymbol{j}}\right)\cdot t \tag{79}$$

, where $E_{\boldsymbol{k}}$ are eigenvalues of $\boldsymbol{\mathcal{H}}$. If phase relations do not exist, or only exist for some components, then we have a mixed state, or a *partially mixed* state. The mixed state is that of a classical object, the pure state is that of a quantum object, and partially mixed state is that of an object in transition from quantum to classical.

An outcome of a single act of measurement is an *event*. The measurement involves collecting sample of events $\{n_{i\in\boldsymbol{G}}\}$. The term *measurement* is thus synonymous to *sampling*. The measurement events on quantum object are formed as a direct product (entanglement) of [more elementary] constituent events, as in example with glove boxes. The entanglement imposes

correlation (phase relations) between measurement events taken in different observation bases, i.e. corresponding to different macroscopic parameters. The constituent events come from the measuring device, from environment, and even from observer memory. A *taken* event sample, decoupled from the measuring device and from the environment, is stored in observer memory. The observation process is illustrated on Figure 12:

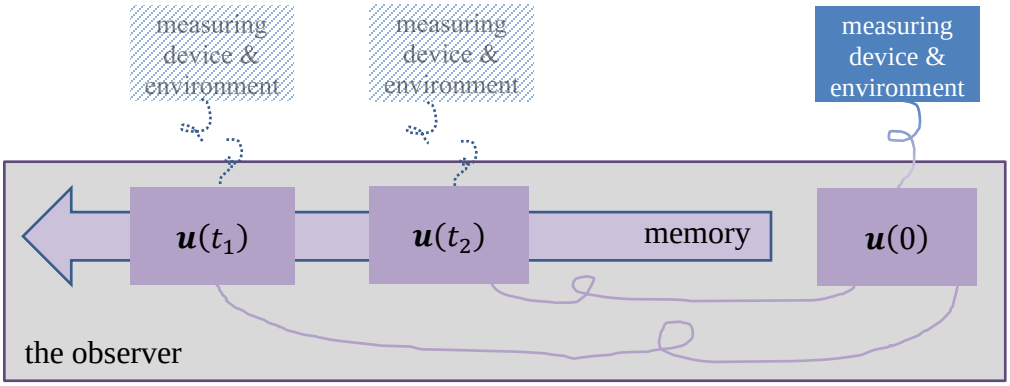

Figure 12

$\boldsymbol{u}(t_1)$, $\boldsymbol{u}(t_2)$ are event samples, taken in observation bases corresponding to parameters t_1, t_2; $\boldsymbol{u}(t_1)$, $\boldsymbol{u}(t_2)$ are decoupled from the measuring device and from environment, and stored in observer memory;
$\boldsymbol{u}(0)$ is the currently captured event sample. The measurement events in $\boldsymbol{u}(0)$ are formed as direct product of constituent events from the measuring device, environment, and memory. The feedback from memory may play a role in emergence of consciousness

The captured event sample $\{n_{i\in\boldsymbol{G}}\}$ can be encoded and stored as, e.g.:

1. Electronic spin configuration in magnetized materials [34]
2. Charge distribution in capacitor elements of charge-coupled devices (CCD) [35]
3. Sequence of nucleotide bases in a DNA strand [36]
4. Neural circuits [37]

It can be proven[3], the knowledge encoded in any form can be construed by a statistical ensemble $\{n_{\boldsymbol{i}\in\boldsymbol{G}}\}$ of orthogonal (uncorrelated) eigenstates (events), with set $\boldsymbol{G}$ being the encoding alphabet.

For a pure state there exists an observation basis (77) in which the measurement would only return event $\boldsymbol{k}$. In such basis, entropy (24) $H_\Omega\big((n_{\boldsymbol{i}\neq\boldsymbol{k}}=0, n_{\boldsymbol{k}}=N);\ N\big)=0$. The state is known, by knowledge amount (23), with confidence (45). In a different observation basis, the measurement sample may consist of events $\{n_{\boldsymbol{i}}>0\}$, with entropy $H_\Omega\big((n_{\boldsymbol{i}});\ N\big)>0$. The sample may not carry the same amount of knowledge, as sample done in $\boldsymbol{k}$ basis, because sample with $H_\Omega\big((n_{\boldsymbol{i}});\ N\big)>0$ does not uniquely identify the state. E.g., a circular polarized light (eigenstate $\boldsymbol{k}$) will produce the same event sample, when measured with linear polarizer, with any orientation of the latter within the plane perpendicular to light propagation, i.e. under any unitary transformation which has $\boldsymbol{k}$ as one of its eigenvectors. For that class of transformations, which

[3] Perhaps a simplistic proof is to consider encoded knowledge as a sequence of yes/no answers in a form of a binary string, which can also be represented as an integer number N. Factorization $\ln N=\sum_i n_i\cdot\ln d_i$ into $\{d_i\}$ primes yields statistical ensemble $\{n_i\}$ where n_i is the exponent of prime d_i in factorization. As prime factors $\{d_i\}$ in factorization are uncorrelated, the associated eigenstates $\{\boldsymbol{i}\}$ are orthogonal.

keep the event sample unchanged, a state vector formalism can be used to extract the knowledge about quantum state from correlations between events taken in different observation bases. The state vector $\boldsymbol{u}$ has to incorporate the correlation mechanism. One way to incorporate correlation is via phase relations between vector components, similar to (79).

The state vector $\boldsymbol{u}$ has to satisfy conditions:

1. $\langle \boldsymbol{u}|\boldsymbol{u}\rangle = 1$; this is the usual normalization requirement
2. Vector $\boldsymbol{u}$ should be invariant, up to a phase factor, with respect to a change in size N of event sample, at least in the limit $N \to \infty$. This is to ensure the conditional measurement probabilities converge to (75)
3. Vector $\boldsymbol{u}$ has to incorporate the relevant macroscopic parameter(s). The variation of parameters should equate to a unitary transformation of observation basis

Vector $\boldsymbol{u}$ is an abstract mathematical construct whose only purpose is to enable correct calculation of conditional probabilities. That's how the wave function should have been treated in a first place. The above considerations lead to the following expression, associated with measurement sample $\{n_{j\in G}\}$, and macroscopic parameter t:

$$|\boldsymbol{u}(t)\rangle = exp\big(-i\cdot\mu\big(N,(p_i)\big)\cdot t\big)\cdot\sum_{j\in G}\sqrt{P_j}exp\big(i\cdot t\cdot\ln P_j\big)\cdot|\boldsymbol{j}\rangle \tag{80}$$

, where $P_j = n_j/N$, and $\mu\big(N,(p_i)\big)$ is (4). The probabilities P_j of different events in the sample are not necessarily equal, because measurement events are not elementary. The energy values $\mathcal{E}_j$ are associated with unconditional probabilities P_j by eq. (9):

$$|\boldsymbol{u}(t)\rangle = \sum_{j\in G}\sqrt{P_j}exp\left(-i\cdot\frac{t\cdot\mathcal{E}_j}{\hbar}\right)\cdot|\boldsymbol{j}\rangle \quad ; \quad \hbar = 1\,\frac{nat}{rad} \tag{81}$$

, where I added conversion constant $\hbar$ because the imaginary argument of $exp(\ \ )$ has to be in $radians$. The correlation coefficient between vectors $\boldsymbol{u}(t_1)$ and $\boldsymbol{u}(t_2)$ is:

$$r = \langle \boldsymbol{u}(t_2)|\boldsymbol{u}(t_1)\rangle = \sum_{j\in G}P_j exp\left(i\cdot\frac{t\cdot\mathcal{E}_j}{\hbar}\right) \tag{82}$$

, where $t = t_2 - t_1$ is the correlation distance. From (82), the coefficient of determination R^2, i.e. the ratio of outcomes in sample 2, which are predictable from sample 1, is:

$$R^2 = |r|^2 = \sum_{i,j\in G}P_iP_j\cos\big(t\cdot\mathcal{E}_{ji}\big) = \left\langle \boldsymbol{P}\right|\cos\left(\frac{t\cdot\boldsymbol{E}}{\hbar}\right)\left|\boldsymbol{P}\right\rangle \tag{83}$$

, where $\boldsymbol{P} = |P_j\rangle$ is the probabilities vector; $\boldsymbol{E} = \mathcal{E}_{ji} = \mathcal{E}_j - \mathcal{E}_i$. Antisymmetric matrix $\boldsymbol{E}$ has two non-zero purely imaginary eigenvalues, which only differ in sign:

$$\mathcal{E}_E = |eigenvalue(\boldsymbol{E})| \quad ; \quad \mathcal{E}_E^2 = trace(\boldsymbol{E}\cdot\boldsymbol{E}^\dagger)/2 = -trace(\boldsymbol{E}^2)/2 \tag{84}$$

Empirically established relations:

$$\left(\frac{\mathcal{E}_E}{M}\right)^2 \fallingdotseq 2h\frac{\mathcal{E}\big((n_i);\ N,(p_i)\big)}{N} \quad ; \quad h = 1\ (nat) \tag{85}$$

$$\mathcal{E}_E^2 = M\cdot(M-1)\cdot\sigma_E^2 \tag{86}$$

, where $\mathcal{E}\big((n_i);\ N,(p_i)\big)$ is energy (6); $\sigma_E^2 = variance(\boldsymbol{E}) = variance(\ln\boldsymbol{P})$. The $\fallingdotseq$ sign in (85) means linear correlation, rather than functional equality. Figure 13 shows correlation between left and right sides of (85) for a number of event samples. In the limit $N \to \infty$ two sides of (85) turn into exact equality.

Eq. (83) is routinely obtained by solving Schrödinger equation for probability of finding an object after time t to be in the same initial state [23]. Evidently, the Born rule (75) is equivalent to coefficient of determination R^2 in statistics, in being a conditional probability measure. The state vector $\boldsymbol{u}(t)$ is the counterpart of wave function. The Schrödinger equation is, as expected[4]:

$$i\hbar\frac{\partial|\boldsymbol{u}\rangle}{\partial t}=\boldsymbol{\mathcal{H}}|\boldsymbol{u}\rangle \qquad \text{, with diagonal form of } \boldsymbol{\mathcal{H}} \text{ being } \mathcal{H}_{jk}=\delta_{jk}\mathcal{E}_k \tag{87}$$

Eq. (83) represents a self-interference of an object at correlation distance t. To generalize for $L>1$ objects, and allow for *dispersion*, and *decoherence*, I rewrite (83) as

$$R^2=\langle\boldsymbol{P}\cdot\boldsymbol{D}|\boldsymbol{D}\cdot P\rangle \tag{88}$$

, where $\boldsymbol{D}$ is the *dispersion matrix*, defined as:

$$\boldsymbol{D}=\frac{1}{L\sqrt{M}}\sum_{l=1}^{L}exp\left(i\cdot\frac{\boldsymbol{\nu}_l\cdot\boldsymbol{E}}{\hbar}\right) \qquad \text{, where} \qquad \boldsymbol{\nu}_l=\left(\nu_{jk}\right)_l \tag{89}$$

Expr. (88) reduces to (83) if $\boldsymbol{\nu}=t\cdot\delta_{jk}$. Matrix $\boldsymbol{\nu}_l$ determines the type of eigenstate dispersion in L correlated objects. Two distinct types of parameter-driven dispersion could be identified:

1. Coherent dispersion:

$$\left(\nu_{jk}\right)_l=t\cdot M\cdot\frac{\left[mnrnd_{jk}\left(d_s,p,M\right)\right]_l}{d_s} \qquad ; \qquad 1\le(j,k)\le M \;;\; 1\le l\le L \tag{90}$$

   , where $d_s\ (nats^{-1})$ is a dispersion parameter. The numeric analysis of (88-90) reveals $R^2(t)$ follows Gaussian profile (Figure 14):

$$R^2(t)=\frac{1}{L\cdot M}+\left(1-\frac{1}{L\cdot M}\right)\cdot exp\left(-\frac{\mathcal{E}_{\boldsymbol{E}}^2t^2}{h^2d_s}\right) \qquad ; \qquad h=1\ (nat) \tag{91}$$

   The dispersion parameter d_s is the property of the device. In case of coherent dispersion, the transition rate $\partial R^2(t)/\partial t\,|_{t=0}=0$.

2. Incoherent dispersion (decoherence):

$$\left(\nu_{jk}\right)_l=M\cdot\left[mnrnd_{jk}\left(t,p,M\right)\right]_l \qquad ; \qquad 1\le(j,k)\le M \;;\; 1\le l\le L \tag{92}$$

   The numeric analysis of (88-89, 92) reveals $R^2(t)$ follows exponential decay (Figure 15):

$$R^2(t)=\frac{1}{L\cdot M}+\left(1-\frac{1}{L\cdot M}\right)\cdot exp\left(-\frac{\mathcal{E}_{\boldsymbol{E}}^2t}{h}\right) \qquad ; \qquad h=1\ (nat) \tag{93}$$

Function $mnrnd(x,p,M)$ in (90, 92) returns $M\times M$ matrix, where each row equals multinomial distribution of x *events* into M buckets, with probability vector p given by (2). The multinomial distribution of x events is generated for each object l, $1\le l\le L$.

The condition for exponential decay (93) is the breakdown of predictable phase relations between constituting particles, i.e. decoherence. The decoherence is imposed by randomly generated $\boldsymbol{\nu}$-matrix (92). The end result of decoherence is the *mixed state*, where probability is spread equally among $L\cdot M$ eigenstates of L dispersed objects.

---

[4] Any continuous dynamics which may be implied by (87) is a detachment from fundamentally discrete nature. The continuous process contradicts quantum postulate, unless it is an …*abstraction, from which no unambiguous information concerning previous or future behavior can be obtained* [28]. I would only provide continuous equations like (87) as a link to conventional theory, not as an advancement of the model

For thermodynamic ensemble, the exponential decay has a different context:

$$K_{\boldsymbol{k}}/K \coloneqq \frac{1}{\Omega_{max}} + (1 - \frac{1}{\Omega_{max}}) \cdot exp(-\lambda \cdot t) \tag{94}$$

, where $K_{\boldsymbol{k}}$ is the number of objects remaining in initial state $\boldsymbol{k}$; K is the total number of objects,

$$\Omega_{max} = exp((H_\Omega)_{max})$$

$$(H_\Omega)_{max} = \ln \Gamma(N+1) - M \cdot \ln \Gamma\left(\frac{N}{M} + 1\right) \tag{95}$$

The exponential decay (94) is driven by transitions of constituting elementary eigenstates. Initially, all objects are in eigenstate $\boldsymbol{k}$, represented by event sample $\{n_{\boldsymbol{i}\neq\boldsymbol{k}} = 0, n_{\boldsymbol{k}} = N\}$, having entropy (24) $H_\Omega = 0$. A transition changes event sample as:

$$\{\dots, n_{\boldsymbol{i}}, \dots, n_{\boldsymbol{k}}, \dots\} \to \{\dots, n_{\boldsymbol{i}} + 1, \dots, n_{\boldsymbol{k}} - 1, \dots\} \tag{96}$$

The transition (96) is accompanied by a change in object entropy H_Ω. The essential feature of a classical decay process is that per-object entropy H is correlated with $K_{\boldsymbol{k}}/K$ as:

$$K_{\boldsymbol{k}}/K \coloneqq exp(-\mathrm{H}) \tag{97}$$

The per-object entropy H is calculated from object entropies (24) $(H_\Omega)_j$ as:

$$\mathrm{H} = -\ln\left[\frac{1}{K}\sum_{j=1}^{K} exp\left(-(H_\Omega)_j\right)\right] \tag{98}$$

The object state can be represented by $(\Omega = N!/\prod_{i\in\boldsymbol{G}} n_i!) > 1$ state vectors $\boldsymbol{u}$, having different phase relationships between constituent events $\{\boldsymbol{i}\}$, due to different values of transformation parameter t. For a given value of transformation parameter, the probability to find object in corresponding state $\boldsymbol{u}$ is $exp(-H_\Omega) = 1/\Omega$.

To prove the correlative relations (94, 97), a numeric analysis of H vs. $-\ln(K_{\boldsymbol{k}}/K)$ vs. $\lambda \cdot t$ has been performed, with wide variation of input parameters. The product $K \cdot \lambda \cdot t$ is the number of transitions (96) randomly distributed across objects. Per object, 1 *transition* equates to 1 nat of information loss. Figure 16 shows values of H/λ, $-\ln(K_{\boldsymbol{k}}/K)/\lambda$, plotted against t. While H and λ are object-dependent, H/λ ratio is not, in the limit $K \to \infty$. The ratio H/λ correlates with classical time, in this analysis represented by independent variable t. It explains why time measures derived from observation of vastly different macroscopic objects, are highly correlative. An illustration of how this correlation breaks down if K is small is the increase in laser linewidth with decrease in number of photons in the mode [38], resulting in less accurate atomic clocks. In terms of time intervals, $\Delta t \coloneqq \Delta\mathrm{H}/\lambda = -\Delta\mathrm{E}/(\lambda \cdot T)$, where $\Delta\mathrm{E}$ is per-object energy loss corresponding to per-object entropy change $\Delta\mathrm{H}$, and T is the temperature introduced in previous section. This relation indicates an accurate clock has to dispense the same amount of energy per cycle. The established correlative relation $\mathrm{H} \coloneqq \lambda \cdot t$ represents the Second Law of Thermodynamics.

Above, energy and entropy are in units of nats. Parameter t is dimensionless. The conversion to SI units is:

$$\frac{\mathcal{E}_{\boldsymbol{E}} t}{\hbar}(radians) = \frac{\mathcal{E}_{\boldsymbol{E}} t\ (J \cdot s)}{\hbar} \tag{99}$$

, where

$$\hbar = 1\ \frac{nat}{rad} = 1.054571817 \cdot 10^{-34}\ \left(\frac{J \cdot s}{rad}\right) \tag{100}$$

, and

$$h = 1\ (nat) = 6.62607015 \cdot 10^{-34}\ (J \cdot s) \tag{101}$$

The conversion (101) is between $nats$ and $(J \cdot s)$. Therefore, energy and time, expressed in SI units, are not independent. If characteristic times of all processes in nature are increased by a factor, then all energies have to decrease by the same factor. There is no separate conversion between energy $\mathcal{E}$ in *nats*, and energy $\mathcal{E}$ in *joules*, or time t in *seconds* and dimensionless parameter t.

The conversion constant h represents an average, per object, quantity of information loss in 1 *transition*. Therefore, a change in amount of knowledge, being a result of a number of transitions, has to satisfy $\Delta H \geq h$. With (93, 85), it leads to the *speed limit* [39]:

$$\mathcal{E}\big((n_i);\ N, (p_i)\big) \cdot t \geq h \cdot N/(2M^2) \tag{102}$$

The R^2 values are dimensionless. They should not depend on units used for arguments in (83, 93). The $\hbar$ conversion constant (100) takes care of that in (83). However, in (93), the resultant expression under $exp()$ is in $nats$, as it should be. If energy is expressed in *joules* (J), and time in *seconds* (s), where would $nats$ under $exp()$ in (93) appear from? There has to be additional conversion parameter added under $exp()$ in (93). This conversion parameter, unlike true conversion constants (100, 101), is a device parameter. With conversion parameter τ added, the expression under $exp()$ in (93), in SI units, becomes:

$$\frac{\mathcal{E}_{\boldsymbol{E}}^2 t}{h} \Rightarrow \frac{\mathcal{E}_{\boldsymbol{E}}^2 \tau}{h^2} t = \lambda t \qquad ; \qquad \lambda = \frac{\mathcal{E}_{\boldsymbol{E}}^2 \tau}{h^2} \tag{103}$$

, where τ $(nats \cdot s)$ is a dimensional device parameter with a meaning of decoherence time [23]. For a classical radiation detector, the expression for τ in (103) is [23]:

$$\tau = \frac{\kappa^2 \Delta\omega}{4\pi^3 c^2 \rho D_\omega} \tag{104}$$

, where c is the speed of light; κ is the refractive index of material; $\Delta\omega$ [*rad/s*] is the spread in object's internal transition frequencies; ρ is the number of correlated objects per unit surface area of the detector; D_ω the dimensionless *scattering rate*. The value $\Delta\omega$ in (104) conceivably is double the standard deviation of $\boldsymbol{E}$-matrix (86), divided by $\hbar$, i.e.:

$$\Delta\omega = 2 \cdot \sigma_{\boldsymbol{E}}/\hbar \tag{105}$$

Then,

$$\tau = \frac{\kappa^2 \sigma_{\boldsymbol{E}}}{\pi^2 h c^2 \rho D_\omega} \qquad ; \qquad \lambda = \frac{\mathcal{E}_{\boldsymbol{E}}^2 \cdot \sigma_{\boldsymbol{E}}}{h^3} \frac{\kappa^2}{\pi^2 c^2 \rho D_\omega} \left(\frac{nats}{s}\right) \tag{106}$$

The expression (106) is a restatement of Fermi's golden rule for transition probability into continuous spectrum near E_f:

$$\lambda = \frac{2\pi}{\hbar} \left|E_{if}\right|^2 \varrho\big(E_f\big) = h\omega^2 \varrho\big(E_f\big) \tag{107}$$

, where $\varrho\big(E_f\big)$ is density of final states, per unit ΔE. By comparing (107) with expression (9) in [23], I get quite simple relation between decoherence time and density of final radiation states:

$$\tau = h\varrho\big(E_f\big) \tag{108}$$

With (106, 108), for classical radiation detector

$$\varrho\big(E_f\big) = \frac{\kappa^2 \sigma_{\boldsymbol{E}}}{\pi^2 h^2 c^2 \rho D_\omega} \tag{109}$$

The left side of (109) purports to be a property of radiation field, while the right side is the property of detector. The fact that seemingly unrelated parameters are connected to each other with only universal constants, is an argument against considering radiation as a standalone entity with properties independent of the measurement context [23].

The model united the seemingly disjoint QM artifacts: Fermi's golden rule and Planck's radiation formula [23], by exposing decoherence (93) as a driving factor in both cases.

References

[1] W. Wislicki, "Thermodynamics of systems of finite sequences," *J. Phys. A: Math. Gen.,* vol. 23, no. 3, p. L121, 1990.

[2] C. Frenzen, "Explicit mean energies for the thermodynamics of systems of finite sequences," *J. Phys. A: Math. Gen.,* vol. 26, no. 9, p. 2269, 1993.

[3] S. Viznyuk, "Thermodynamic properties of finite binary strings," *arXiv:1001.4267 [cs.IT],* 2010.

[4] R. Albert and A.-L. Barabási, "Statistical mechanics of complex networks," *Rev. Mod. Phys.,* vol. 74, pp. 47-97, 2002.

[5] G. Bianconi and A.-L. Barabási, "Bose-Einstein condensation in complex networks," *arXiv:cond-mat/0011224 [cond-mat.dis-nn],* 2000.

[6] M. Bouchaud, "Wealth Condensation in a simple model of economy," *Physica A Statistical Mechanics and its Applications,* vol. 282, p. 536, 2000.

[7] S. Sieniutycz and P. Salamon, Finite-Time Thermodynamics and Thermoeconomics, Taylor & Francis, 1990.

[8] J. Chan, T. Alegre, A. Safavi-Naeini, J. Hill, A. Krause, S. Groeblacher, M. Aspelmeyer and O. Painter, "Laser cooling of a nanomechanical oscillator into its quantum ground state," *arXiv:1106.3614 [quant-ph],* 06 2011.

[9] A.-L. Barabási and E. Bonabeau, "Scale-Free Networks," *Scientific American,* vol. 288, pp. 50-59, 2003.

[10] R. Penrose, "On Gravity's Role in Quantum State Reduction," *General Relativity and Gravitation,* vol. 28, no. 5, pp. 581-600, 1996.

[11] M. Jammer, "The Conceptual Development of Quantum Mechanics," in *The History of Modern Physics*, Tomash, 1989.

[12] S. Viznyuk, "New QM framework," ResearchGate.net, 2014. [Online]. Available: https://www.researchgate.net/publication/293992646_New_QM_framework.

[13] S. Viznyuk, "Shannon's entropy revisited," *arXiv:1504.01407 [cs.IT],* 03 2015.

[14] K. Yamanaka, S. Kawano and K. Y., "Constant Time Generation of Integer Partitions," *IEICE Transactions on Fundamentals of Electronics, Communications and Computer Sciences,* Vols. E90-A, no. 5, pp. 888-895, 2007.

[15] S. Viznyuk, "OEIS sequence A210237," 2012. [Online]. Available: https://oeis.org/A210237. [Accessed 21 04 2015].

[16] D. Collins, "Entropy Maximizations on Electron Density," *Z. Naturforsch,* vol. 48a, pp. 68-74, 1993.

[17] C. Forbes, M. Evans, N. Hastings and B. Peacock, Statistical Distributions, Fourth Edition, Hoboken, NJ, USA: John Wiley & Sons, Inc., 2010.

[18] D. J. Griffiths, Introduction to Quantum Mechanics, 2nd ed., Pearson Education, Inc., 2005.

[19] N. Sloane, "OEIS sequence A003136," 1991. [Online]. Available: https://oeis.org/A003136. [Accessed 2015].

[20] I. Vapnyarskii, "Lagrange multipliers," in *Encyclopedia of Mathematics,* Springer, 2001.

[21] M. S. I. A. Abramowitz, "6.3 psi (Digamma) Function," in *Handbook of Mathematical Functions with Formulas, Graphs, and Mathematical Tables*, New York: Dover, 1972, p. 258–259.

[22] K. Huang, Statistical Mechanics, John Wiley & Sons, 1987.

[23] S. Viznyuk, "Planck's law revisited," Academia.edu, 2017. [Online]. Available: https://www.academia.edu/35548486/Plancks_law_revisited.

[24] P. Jordan and W. Pauli, "Zur Quantenelektrodynamik ladungsfreier Felder," *Zeitschrift für Physik,* vol. 47, no. 3, pp. 151-173, 1928.

[25] G. Grundler, "The zero-point energy of elementary quantum fields," *arXiv:1711.03877 [physics.gen-ph],* Novermber 2017.

[26] J. Bell, "Against 'measurement'," *Physics World,* August 1990.

[27] J. Wheeler and W. Zurek, Quantum Theory and Measurement, Princeton University Press, NJ, 1983.

[28] N. Bohr, "The Quantum Postulate and the Recent Development of Atomic Theory," *Nature,* pp. 580-590, 14 April 1928.

[29] M. Tegmark, "The Interpretation of Quantum Mechanics: Many Worlds or Many Words?," *arXiv:quant-ph/9709032,* 1997.

[30] A. Einstein, N. Rosen and B. Podolsky, "Can Quantum-Mechanical Description of Physical Reality Be Considered Complete," *Phys. Rev.,* vol. 47, p. 777, 1935.

[31] H. Everett, "Relative State Formulation of Quantum Mechanics," *Reviews of Modern Physics,* vol. 29, pp. 454-462, 1957.

[32] D. Bohm, "A suggested interpretation of the quantum theory in terms of hidden variables," *Phys. Rev.,* vol. 85, pp. 166-179, 1952.

[33] R. Haag, "On Quantum Field Theories," *Dan. Mat. Fys. Medd.,* vol. 29, no. 12, pp. 1-37, 1955.

[34] C. Chappert, A. Fert and F. Van Dau, "The emergence of spin electronics in data storage," *Nature Mater,* vol. 6, no. 11, p. 813–823, 2007.

[35] M. Lesser, "Charge coupled device (CCD) image sensors," in *High Performance Silicon Imaging, Fundamentals and Applications of CMOS and CCD Sensors*, Woodhead Publishing, 2014, pp. 78-97.

[36] M. Mansuripur, "DNA, Human Memory, and the Storage Technology of the 21st Century," *Proceedings of SPIE,* vol. 4342, pp. 1-29, 2002.

[37] T. Kitamura, S. Ogawa, D. S. Roy, T. Okuyama, M. Morrissey, L. Smith, R. Redondo and S. Tonegawa, "Engrams and circuits crucial for systems consolidation of a memory," *Science,* vol. 356, no. 6333, pp. 73-78, 2017.

[38] H. Wiseman, "The ultimate quantum limit to the linewidth of lasers," arXiv:quant-ph/9903082, 1999. [Online]. Available: https://arxiv.org/abs/quant-ph/9903082.

[39] S. Deffner and S. Campbell, "Quantum speed limits: from Heisenberg's uncertainty principle to optimal quantum control," *arXiv:1705.08023 [quant-ph],* 16 10 2017.

[40] S. J. Strickler, "Electronic Partition Function Paradox," *Journal of Chemical Education,* vol. 43, no. 7, pp. 364-366, 1966.

[41] S. Viznyuk, "OEIS sequence A210238," 2012. [Online]. Available: http://oeis.org/A210238. [Accessed 21 04 2015].

$N = 1000;\ M = 2;$ $\{p_i\} = \{\frac{1}{2}, \frac{1}{2}\}$		$N = 900;\ M = 3;$ $\{p_i\} = \{\frac{1}{3}, \frac{1}{3}, \frac{1}{3}\}$		$N = 600;\ M = 5;$ $\{p_i\} = \{\frac{1}{5}, \frac{1}{5}, \frac{1}{5}, \frac{1}{5}, \frac{1}{5}\}$		$N = 189;\ M = 7;$ $\{p_i\} = \{\frac{1}{7}, \frac{1}{7}, \frac{1}{7}, \frac{1}{7}, \frac{1}{7}, \frac{1}{7}, \frac{1}{7}\}$	
$\mathcal{E}$	$g(\mathcal{E}; N, \{p_i\})$	$\mathcal{E}$	$g(\mathcal{E}; N, \{p_i\})$	$\mathcal{E}$	$g(\mathcal{E}; N, \{p_i\})$	$\mathcal{E}$	$g(\mathcal{E}; N, \{p_i\})$
0.000000	1	0.000000	1	0.000000	1	0.000000	1
0.001998	2	0.003328	6	0.008299	20	0.036368	42
0.007992	2	0.009972	3	0.016598	30	0.072735	210
0.017982	2	0.009994	3	0.024828	30	0.107827	105
0.031968	2	0.013311	6	0.024966	30	0.109103	140
0.049951	2	0.023262	6	0.033127	20	0.110476	105
0.071930	2	0.023328	6	0.033196	20	0.144194	420
0.097905	2	0.029951	6	0.033265	20	0.145567	42
0.127878	2	0.039846	3	0.041495	120	0.146843	420
0.161847	2	0.040023	3	0.049521	20	0.180562	105
0.199813	2	0.043196	6	0.050072	20	0.181935	840
0.241778	2	0.043329	6	0.057889	60	0.183211	105
0.287740	2	0.053246	6	0.058024	30	0.213187	140
0.337700	2	0.063064	6	0.058162	30	0.215653	105
0.391659	2	0.063396	6	0.058302	60	0.218302	1260
0.449618	2	0.069775	6	0.066188	60	0.220951	105
0.511576	2	0.069997	6	0.066393	30	0.223804	140
0.577534	2	0.083198	6	0.066601	60	0.249555	210
0.647492	2	0.089556	3	0.074556	60	0.250928	210
0.721452	2	0.090154	3	0.074696	20	0.253394	630
[...]	[...]	[...]	[...]	[...]	[...]	[...]	[...]
640.1354	2	952.5446	6	929.0220	30	333.7789	105
644.8379	2	955.9414	3	929.4275	60	334.1844	210
649.6592	2	956.3468	6	930.8138	20	335.5707	42
654.6150	2	957.7331	6	934.0276	20	337.6184	140
659.7260	2	962.0473	6	934.7208	60	338.3115	210
665.0203	2	963.1459	6	935.8194	20	339.4101	42
670.5388	2	968.1543	3	940.4212	30	342.8495	105
676.3459	2	968.8474	6	941.1144	20	343.5426	42
682.5595	2	974.9556	6	946.8165	20	348.0859	42
689.4673	2	981.7580	3	953.2134	5	353.3277	7

Table 1

$\mathcal{E}$, $g(\mathcal{E}; N, \{p_i\})$ value pairs calculated from (6) for four sets of parameters $N, \{p_i\}$ using [14] algorithm for finding partitions $\{n_i\}$ of integer N into $\leq M$ parts. For each partition $\{n_i\}$ I calculated the value of $\mathcal{E}$ and multiplicity $D(\mathcal{E}; N, M)$ of multinomial coefficient in (1) [41]. Finally, $g(\mathcal{E}; N, \{p_i\}) = sum(D)$ for each distinct value of $\mathcal{E}$ produced the results for the table. I display the first 20 and the last 10 records from the table.

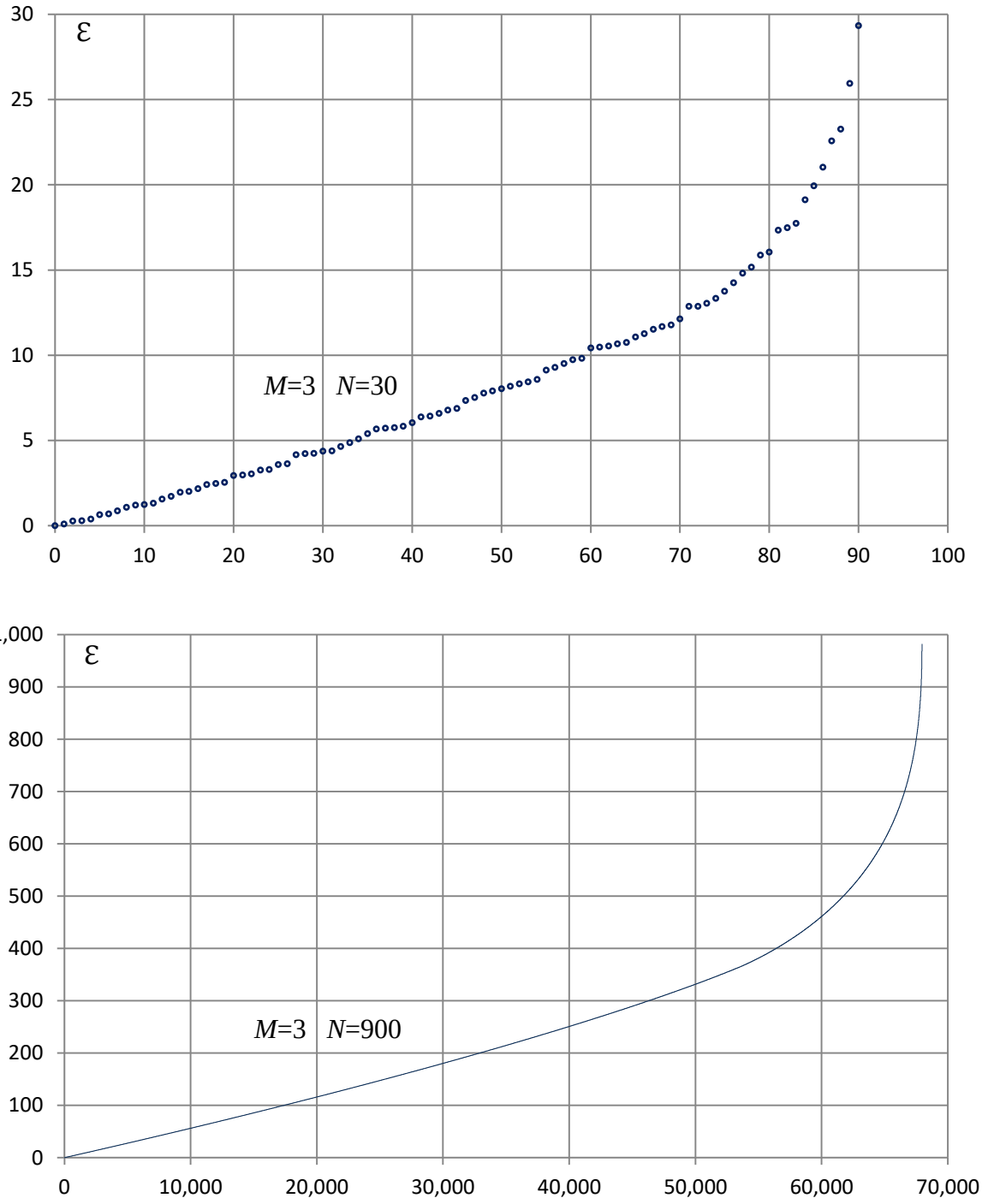

Figure 1

Distinct values of $\mathcal{E}$ in increasing order calculated from (6) with (2), using [14] algorithm for finding partitions $\{n_i\}$ of integer N into $\leq M$ parts. The values of M and N are given on the graphs. The graphs represent complete set of distinct values of $\mathcal{E}$ for the given values of M and N. The graphs demonstrate close to linear dependence of $\mathcal{E}$ on "quantum number" in the vicinity of equilibrium $\mathcal{E} = 0$. This is a characteristic feature of a sample with cardinality $M = 3$. Away from equilibrium the linear behavior is violated as interval $\Delta\mathcal{E}$ between energy levels begins to grow to reach $(\Delta\mathcal{E})_{max} = \ln N$

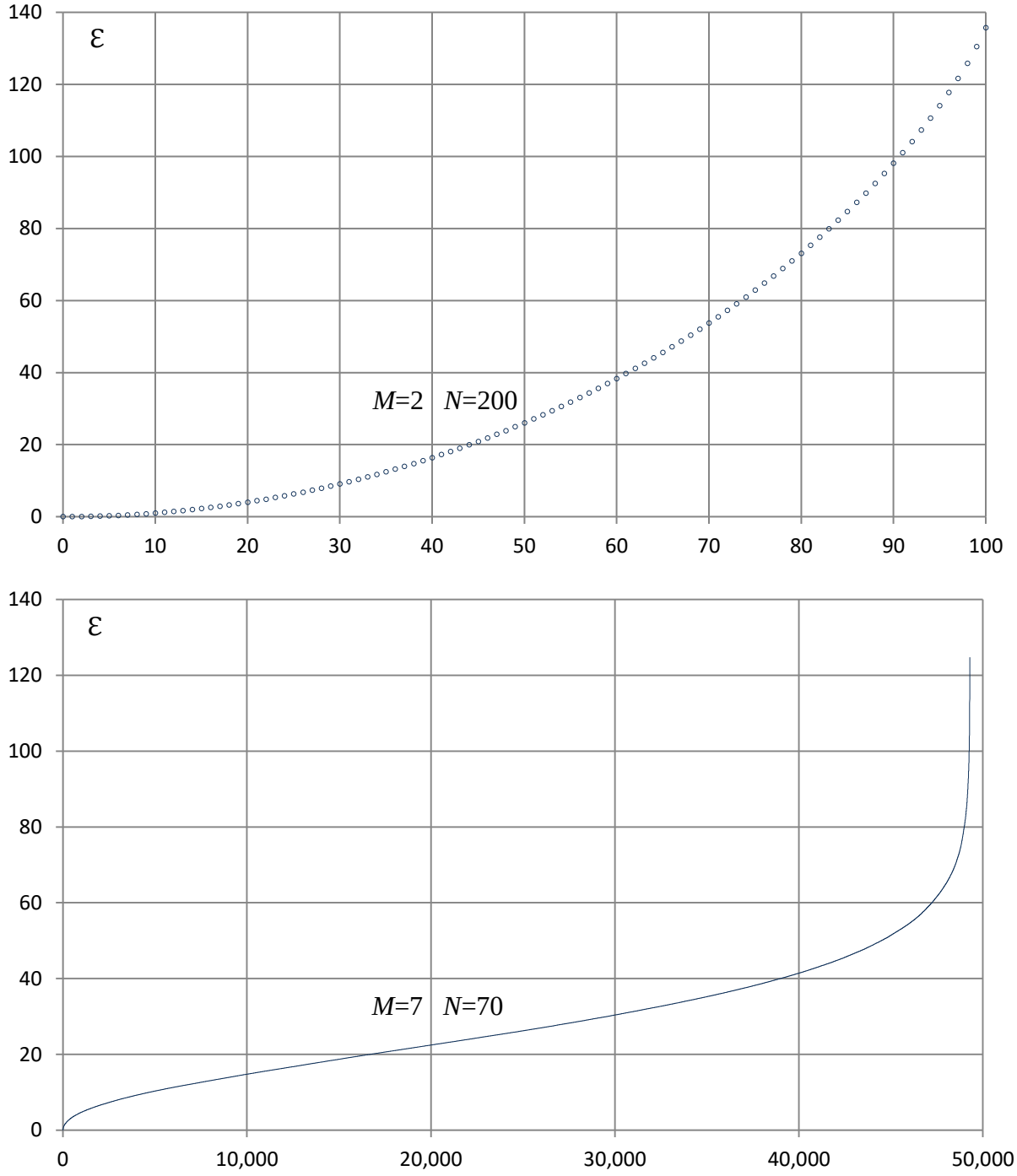

Figure 2

Distinct values of $\mathcal{E}$ in increasing order calculated from (6) with (2), using [14] algorithm for finding partitions $\{n_i\}$ of integer N into $\leq M$ parts. The values of M and N are given on the graphs. The graphs represent complete set of distinct values of $\mathcal{E}$ for the given values of M and N.

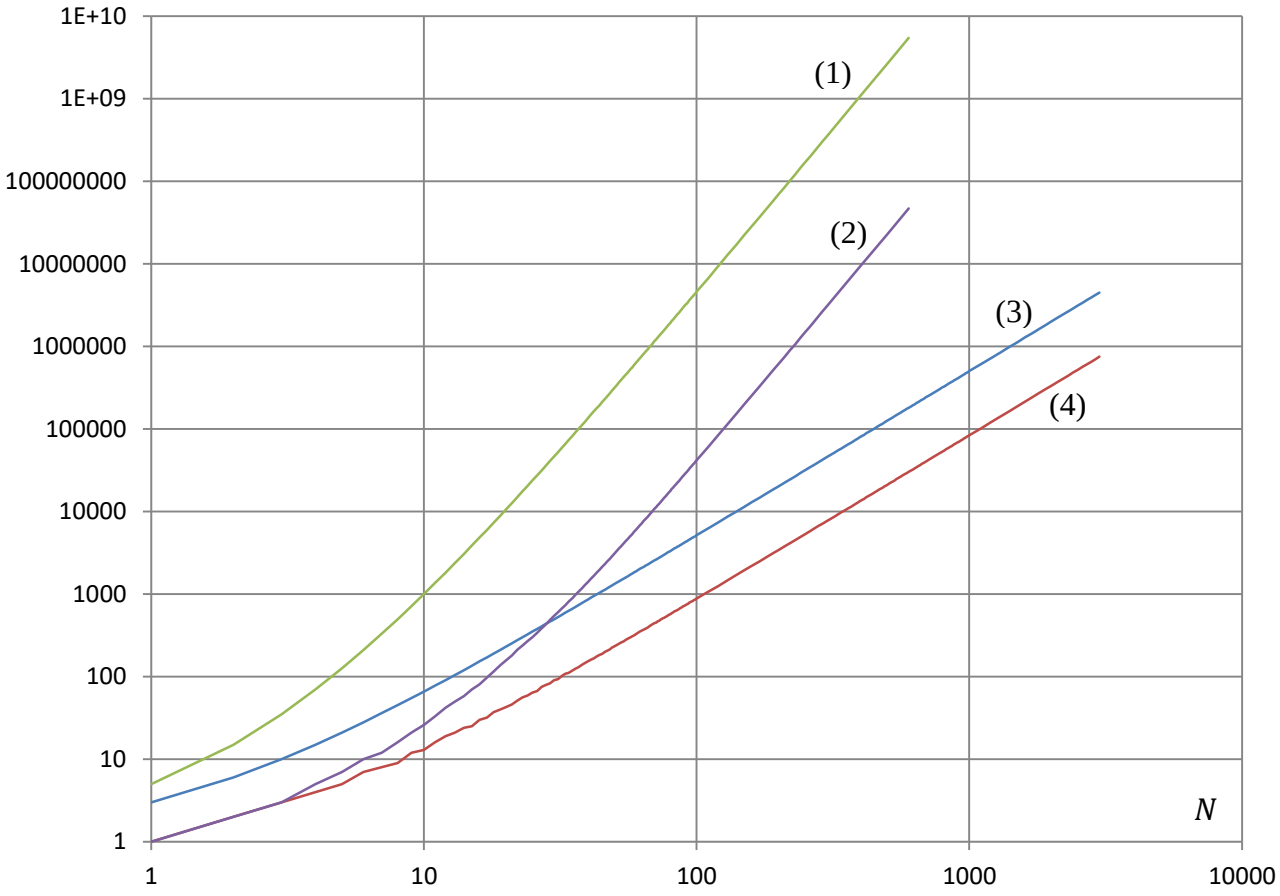

Figure 3

The total number $F(N,M)$ of distinct event samples (curves 1, 3), and the total number $\sum_{\{\mathcal{E}\}} 1$ of distinct $\{\mathcal{E}\}$ values (curves 2, 4) as functions of N for two sets of probabilities (5):

1. $F(N,M)$ for $M = 5$
2. $\sum_{\{\mathcal{E}\}} 1$ for $M = 5$
3. $F(N,M)$ for $M = 3$
4. $\sum_{\{\mathcal{E}\}} 1$ for $M = 3$

The values on curve 1 are by factor $M! = 5!$ greater than on curve 2 as $N \to \infty$. The values on curve 3 are by factor $M! = 3!$ greater than on curve 4 as $N \to \infty$.

Using Stirling's approximation for large N in (11) one can show the curves grow proportionally to N^{M-1} as $N \to \infty$

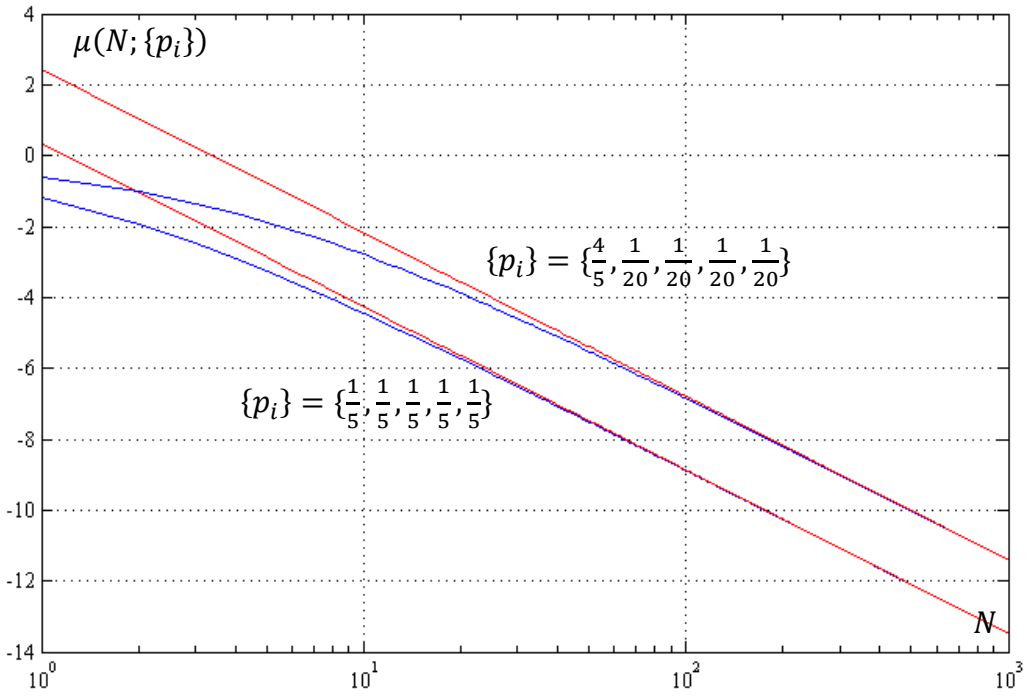

Figure 4

Function $\mu(N;\{p_i\})$ calculated for two sets of probabilities $\{p_i\}$. Blue lines were calculated using formula (4). Red lines were calculated using thermodynamic limit approximation (15)

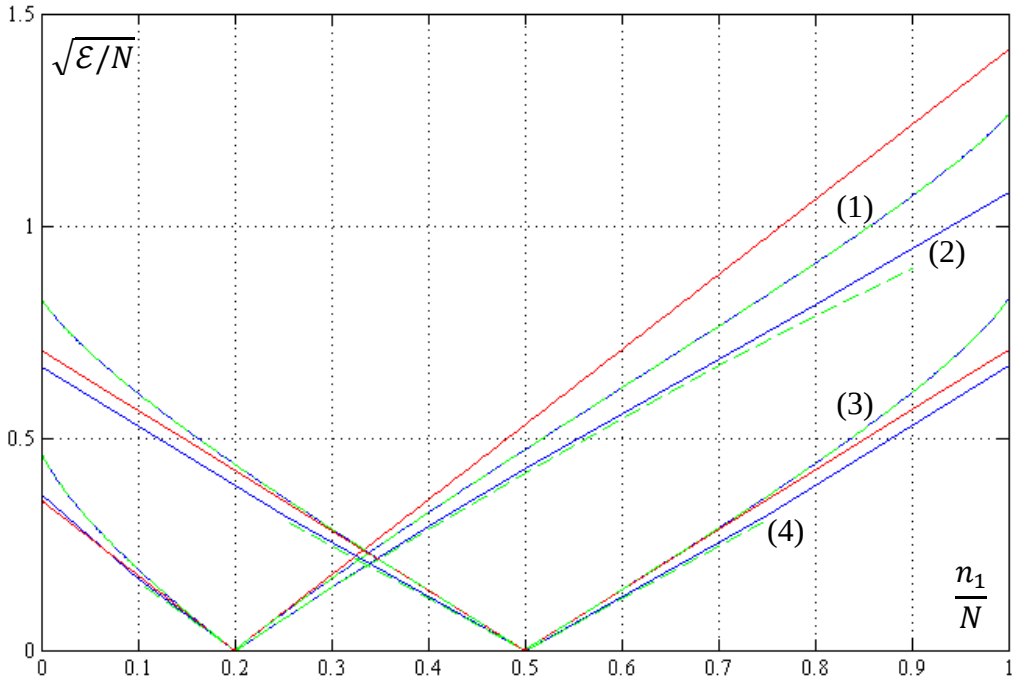

Figure 5

Values of $\sqrt{\mathcal{E}/N}$ calculated as a function of n_1/N with probabilities (2) for four sets of parameters:

1. $M = 5;\ N = 1000$
2. $M = 5;\ N = 10$
3. $M = 2;\ N = 1000$
4. $M = 2;\ N = 4$

Blue lines were calculated using formula (6). Green dash lines were calculated using thermodynamic limit approximation (16). Red lines were calculated using quadratic form (22) approximation. For a given value of n_1 the values $\{n_{i>1}\}$ were distributed proportionally to corresponding probabilities $\{p_{i>1}\}$. For large value of $N = 1000$ the blue lines and green dash lines overlap closely as seen on curves 1 and 3. For small values of N the thermodynamic limit approximation is not accurate, and blue lines differ from green dash lines as seen on curves 2 and 4. Red lines overlap with blue lines in close proximity to the minimum (7) of $\mathcal{E}$.

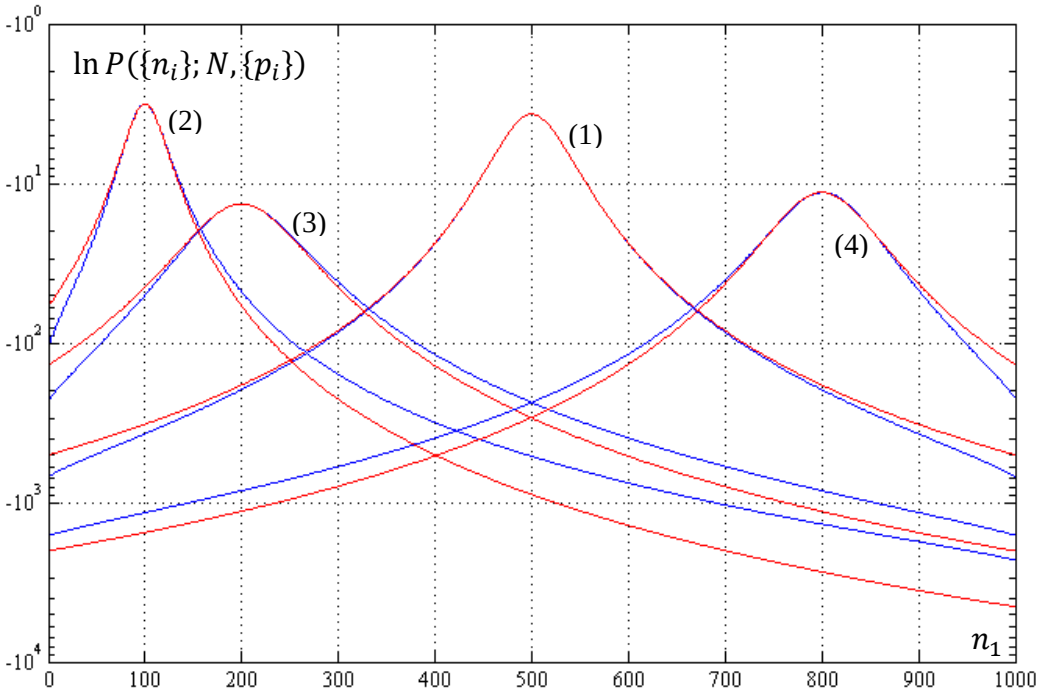

Figure 6

Values of $\ln P(\{n_i\}; N, \{p_i\})$ calculated as a function of n_1 for $N = 1000$ and four sets of probabilities $\{p_i\}$

1. $\{p_i\} = \left\{\frac{1}{2}, \frac{1}{2}\right\}$
2. $\{p_i\} = \left\{\frac{1}{10}, \frac{9}{10}\right\}$
3. $\{p_i\} = \left\{\frac{1}{5}, \frac{1}{5}, \frac{1}{5}, \frac{1}{5}, \frac{1}{5}\right\}$
4. $\{p_i\} = \{\frac{4}{5}, \frac{1}{20}, \frac{1}{20}, \frac{1}{20}, \frac{1}{20}\}$

Blue lines were calculated using formula (1). Red lines were calculated using multivariate normal approximation (25). For the given value of n_1 the distribution of values $\{n_{i>1}\}$ is proportional to the corresponding probabilities $\{p_{i>1}\}$

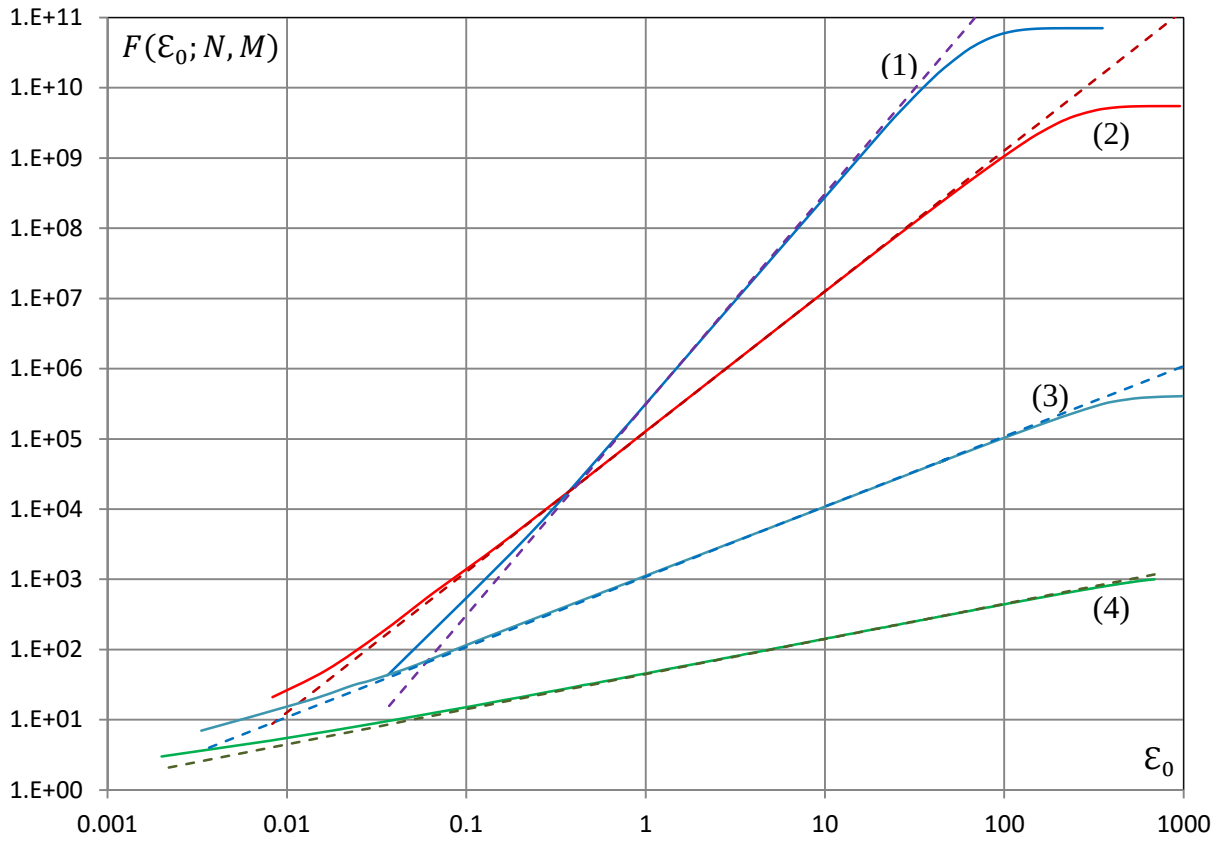

Figure 7

The number $F(\mathcal{E}_0; N, M)$ of object states having $\mathcal{E} \leq \mathcal{E}_0$ as a function of $\mathcal{E}_0$ for three sets of the parameters and probabilities (2):

1. $M = 7;\ N = 189$
2. $M = 5;\ N = 600$
3. $M = 3;\ N = 900$
4. $M = 2;\ N = 1000$

Solid lines are the results of calculation using formulas (1, 6). Dash lines represent thermodynamic limit approximation (33). The graphs show thermodynamic limit provides the better approximation the larger is the ratio N/M. Solid lines level off close to $\mathcal{E}_{max}$ because density of states per interval $d\mathcal{E}$ decreases near $\mathcal{E}_{max}$ due to non-spherical $\mathcal{E}$-domain boundary. The boundary is defined by $\sum_{i \in \boldsymbol{G}} n_i = N\ ;\ n_{\boldsymbol{i}} \geq 0\ \forall\ \boldsymbol{i} \in \boldsymbol{G}$

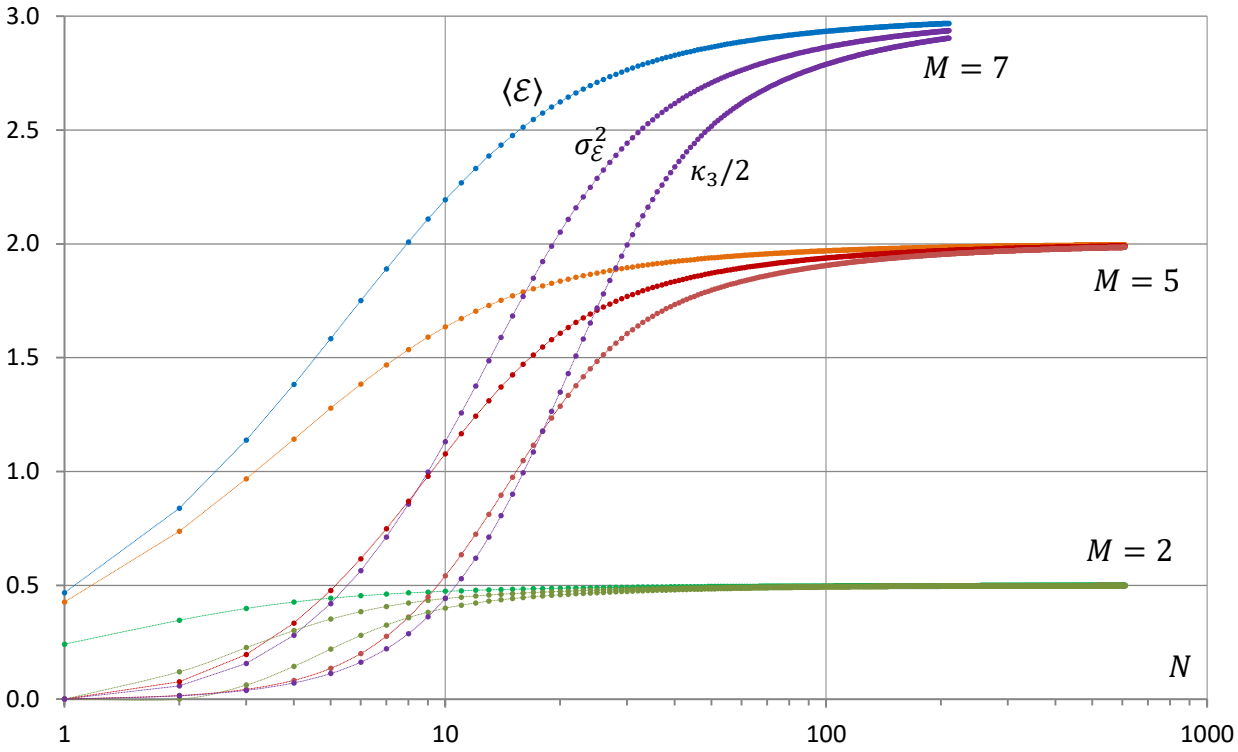

Figure 8

The mean value $\langle \mathcal{E} \rangle$, the variance $\sigma_{\mathcal{E}}^2$, and the third moment κ_3 vs. sample size N for three values of M and probabilities (2). The graphs have been calculated using expressions (39-41) with probability mass function (1). The value of the third moment κ_3 is reduced by a factor of 2 to show its asymptotic behavior comparing with $\langle \mathcal{E} \rangle$ and $\sigma_{\mathcal{E}}^2$. For each set of parameters, the curves approach $(M-1)/2$ values as $N \cdot p_i \to \infty$

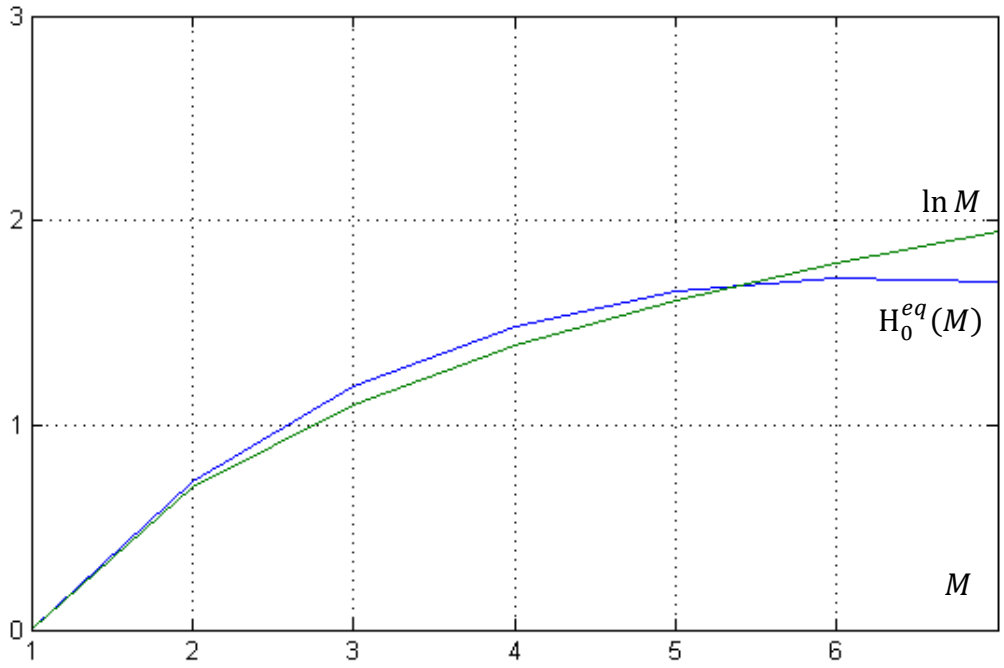

Figure 9

Comparison of $\mathrm{H}_0^{eq}(M)$ in (68) with $\ln M$

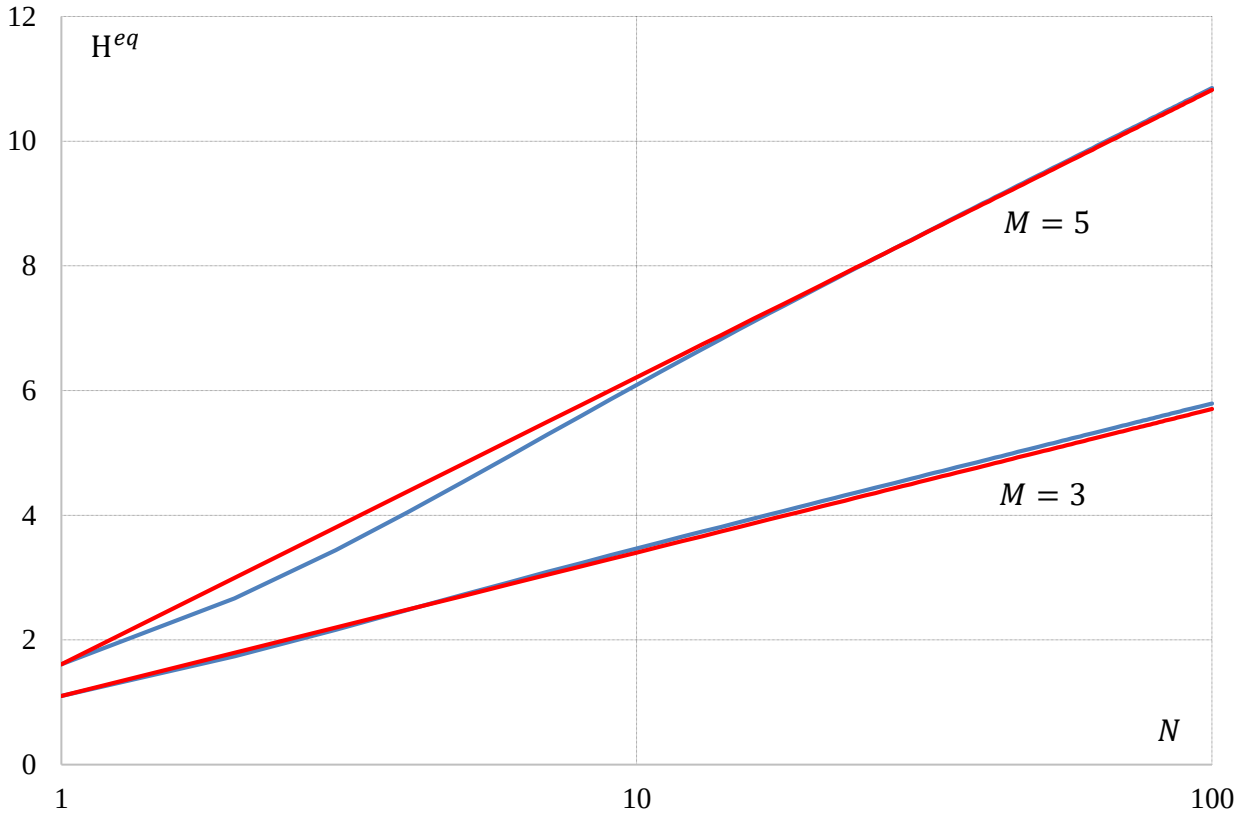

Figure 10

In blue is the thermodynamic equilibrium entropy H^{eq} of a standalone object calculated from $H^{eq} = -\sum_{\{k\}} p_{\boldsymbol{k}} \cdot \ln p_{\boldsymbol{k}}$, where $p_{\boldsymbol{k}}$ is given by (66). In red is the thermodynamic equilibrium entropy calculated from (69).
Two sets of graphs are for two values of M.

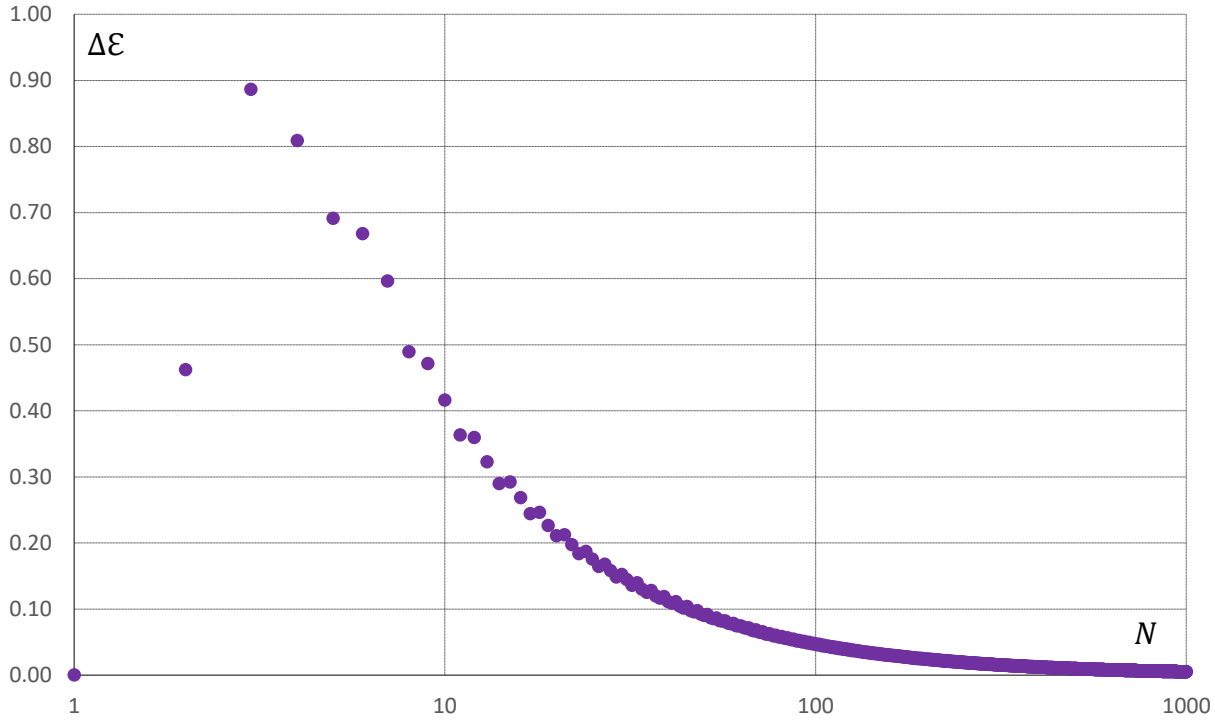

Figure 11

Difference $\Delta\mathcal{E}$ between adjacent energy levels (6), averaged over distinct event samples with given value of N, and $M = 3$. The curve is approximated by (70) as $N \to \infty$

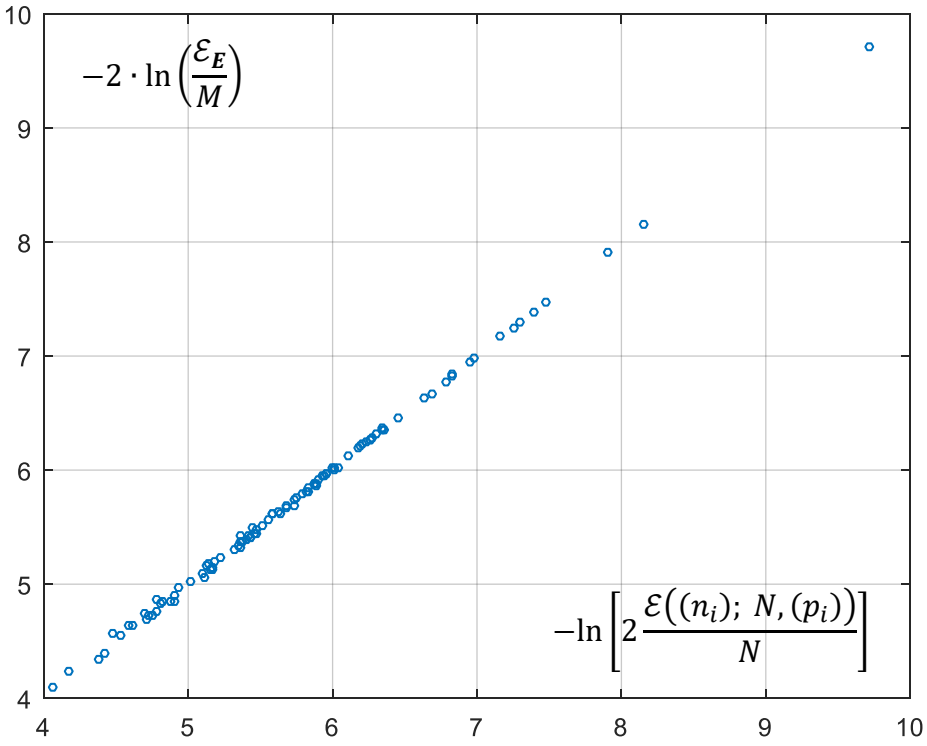

Figure 13

The $-\ln(\quad)$ of left and right sides of (85), showing high degree of linear correlation. The graph was produced with MATLAB code:
http://phystech.com/download/e2correlation.m
with parameters: $M = 5;\ N = 10000$

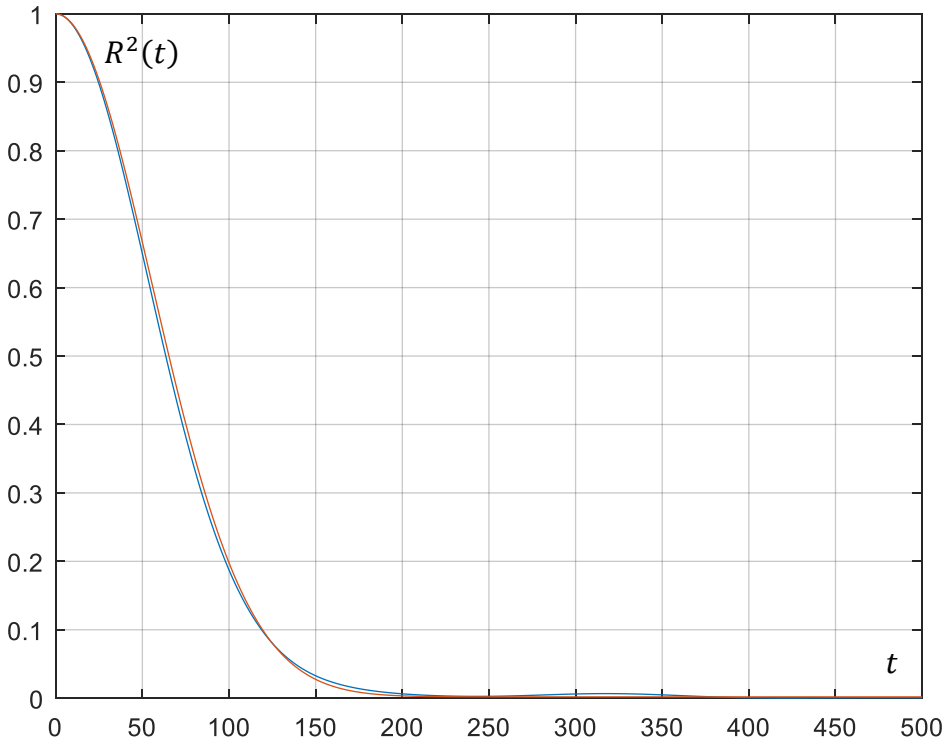

Figure 14

Blue line is calculation of $R^2(t)$ from (88-90) with parameters: $M = 5$; $L = 100$; $N = 1000$; $d_s = 1000$, and event sample $\{n_i\}$ generated with multinomial *pmf* (1).

Red line is Gaussian profile (91), where $\mathcal{E}_E = 0.4035$ has been computed from event sample $\{n_i\}$ generated for blue line.

The MATLAB code used in calculation:
http://phystech.com/download/gaussian_dispersion.m

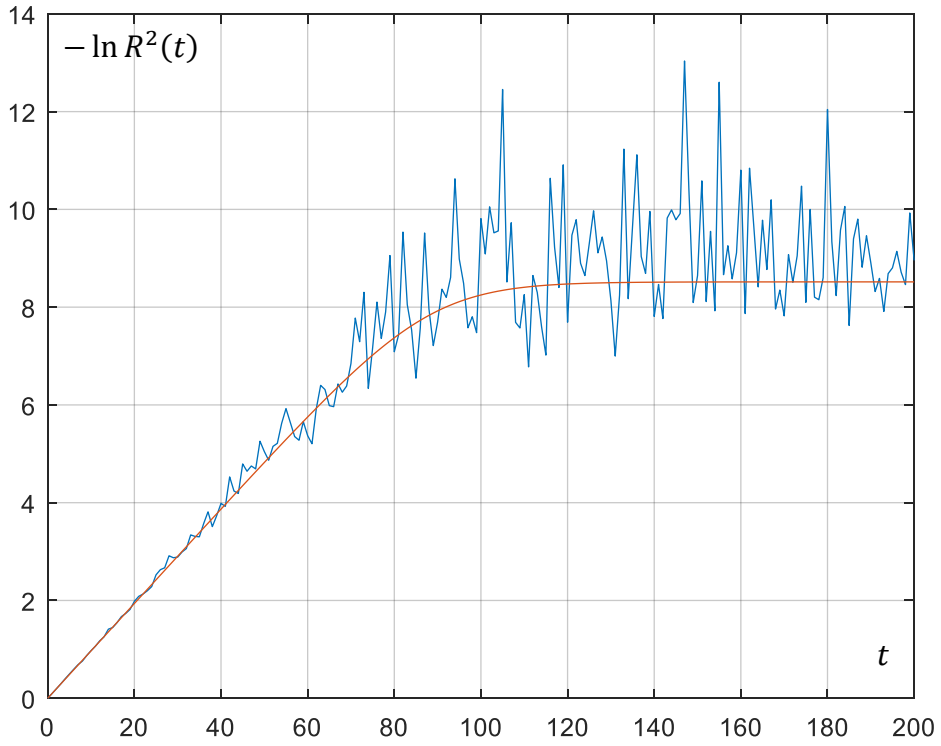

Figure 15

Blue line is calculation of $-\ln R^2(t)$ from (88-89, 92) with parameters: $M = 5\,;\ L = 1000\,; N = 1000$, and event sample $\{n_i\}$ generated with multinomial *pmf* (1)

Red line is exponential decay (93), where $\mathcal{E}_E = 0.3114$ has been computed from event sample $\{n_i\}$ generated for blue line.

The MATLAB code used in calculation:
http://phystech.com/download/exponential_dispersion.m

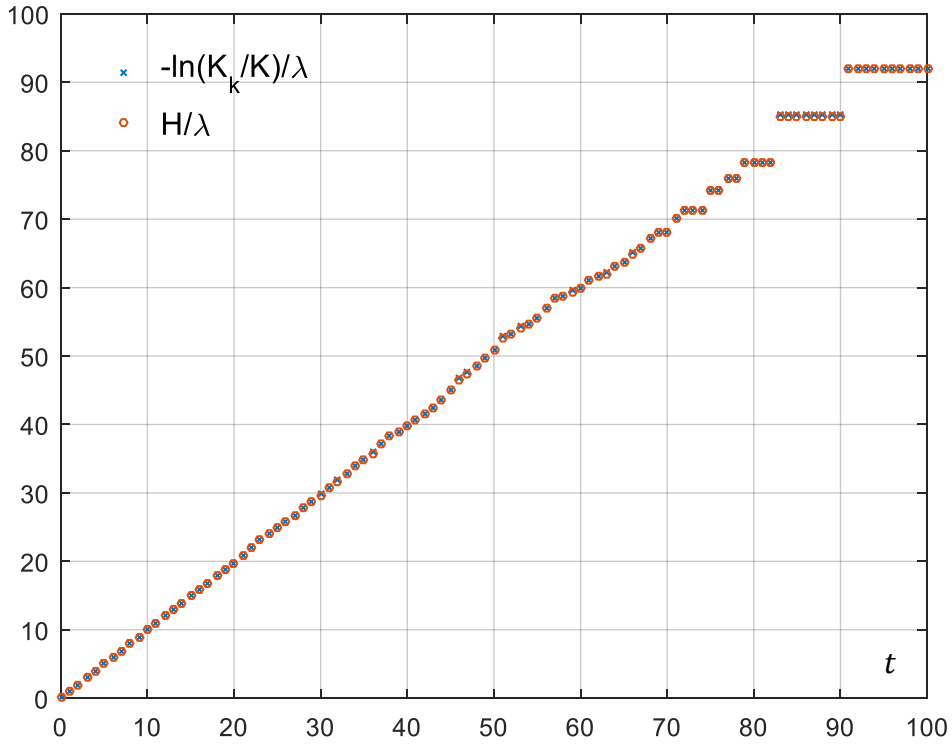

Figure 16

Blue crosses, visible inside red circles, are values of $-\ln(K_{\boldsymbol{k}}/K)/\lambda$, where K is the total number of objects; λ is the per-object *information outflow rate*; $K_{\boldsymbol{k}}$ is the number of objects remaining in initial mode $\boldsymbol{k}$ after $K \cdot \lambda \cdot t$ transitions (96). Red circles are the corresponding values of H/λ, where H is calculated as (98) with (24). Transitions (96) are randomly generated at a rate of λ transitions per object per t interval.

The MATLAB code used in calculation:
http://phystech.com/download/time_entropy.m
with parameters:
$M = 7\ ;\ K = 10000\ ;\ N = 1000\ ;\ \lambda = 0.1$